https://doi.org/10.5194/egusphere-2024-85
Preprint. Discussion started: 19 January 2024

INTERSEISMIC AND LONG-TERM DEFORMATION OF SOUTHEASTERN SICILY DRIVEN BY THE IONIAN SLAB ROLL-BACK

Amélie Viger[1*], Stéphane Dominguez[1*], Stéphane Mazzotti[1], Michel Peyret[1], Maxime Henriquet[2], Giovanni Barreca[3*], Carmelo Monaco[3], Adrien Damon[1]

(1) Géosciences Montpellier, Université de Montpellier, CNRS, Montpellier, France
(2) Aix-Marseille Université, CEREGE, Aix-en-Provence, France
(3) Dipartimento di Scienze Biologiche, Geologiche e Ambientali, Sezione di Scienze della Terra, Università di Catania, Catania, Italy
*e-mail, amelie.viger.geo@gmail.com, stephane.dominguez@umontpellier.fr, giobarre@unict.it

Key Points

- Recent satellite geodetic data shed new light on the origin of the active deformations affecting Southeastern Sicily.
- Several deformation processes, including crustal flexure and faulting, are investigated to determine the most reliable mechanical explanation.
- Seismic cycle, surface, and crustal deformations of Southeastern Sicily are mainly driven by the southward migration of the Ionian slab roll-back.

Abstract:

New satellite geodetic data challenge our knowledge of the deformation mechanisms driving the active deformations affecting Southeastern Sicily. The PS-InSAR measurements evidence a generalized subsidence and an eastward tilting of the Hyblean Plateau combined with a local relative uplift along its eastern coast. In order to find a mechanical explanation for the present-day strain field, we investigate short and large-scale surface-to-crustal deformation processes. Geological and geophysical data suggest that the southward migration of the Calabrian subduction could be the causative geodynamic process. We evaluate this hypothesis using flexural modeling and show that the overloading of the Calabrian accretionary prism, combined with the downward pull force induced by the Ionian slab roll-back, are capable of flexuring the adjacent Hyblean continental crust, explaining

https://doi.org/10.5194/egusphere-2024-85
Preprint. Discussion started: 19 January 2024

the measured large-scale subsidence and eastward bending of the Hyblean Plateau. To explain the short-scale relative uplift evidenced along the eastern coast, we perform elastic modeling on identified or inferred onshore and offshore normal faults. We also investigate the potential effects of other deformation processes including upwelling mantle flow, volcanic deflation, and hydrologic loading. Our results enable us to propose an original seismic cycle model for Southeastern Sicily, linking the current interseismic strain field and the available long-term deformation data. This model is mainly driven by the southward migration of the Ionian slab roll-back which induces a downward force capable to flexure the Hyblean crust.

Keywords: Southeastern Sicily, surface deformation, PS-InSAR, slab roll-back, slab pull, crustal/lithospheric flexure, extrado faulting, seismic cycle, numerical modeling

1. Introduction

Geodetic measurements, instrumental seismicity, onshore/offshore geology, and geophysics, all indicate that Southeastern Sicily is actively deforming (e.g., Anzidei *et al.*, 2021; Azzaro and Barbano, 2000; Mastrolembo *et al.*, 2014; Meschis *et al.*, 2020). This region also suffered the most powerful and devastating earthquake reported in the Italian seismicity catalog, the 1693 Mw~7.4 Val-di-Noto earthquake, which occurred along the eastern margin of the Hyblean Plateau (e.g., Bianca *et al.*, 1999; Billi *et al.*, 2010; Gutscher *et al.*, 2006; Scicchitano *et al.*, 2022). The current geologic and tectonic framework is in line with the Cenozoic geodynamic evolution of the Central Mediterranean (Figure 1), but also appears to be influenced by the Mesozoic pre-structuration of this region (e.g., Carminati and Doglioni, 2005; Frizon de Lamotte *et al.*, 2011; Henriquet *et al.*, 2020; Van Hinsbergen *et al.*, 2020). In the Late Cretaceous (~80 Myr), the Africa/Eurasia plates conver-

https://doi.org/10.5194/egusphere-2024-85
Preprint. Discussion started: 19 January 2024

gence initiated the oceanic subduction of the Alpine Tethys under the Apulia-Adria micro-continent (e.g., Handy *et al.*, 2010). Since the Oligocene (~30 Myr), the ~~Alpine Tethys~~ subduction has experienced slab roll-back, causing the drifting of continental micro-blocks, detached from the Iberia plate and the opening of back-arc basins over the Mediterranean realm (e.g., Carminati *et al.*, 2012; Gueguen *et al.*, 1998; Rosenbaum *et al.*, 2002). During the Mio-Pliocene (10-5 Myr), the collision of the ~~retreating~~ Calabrian-Peloritan ~~subduction~~ arc ~~and accretionary wedge~~ with the Northern African passive margin led to the formation of the Sicilian fold-and-thrust belt (e.g., Henriquet *et al.*, 2020). During the Plio-Pleistocene (5-2 Myr), the Calabrian subduction continued strongly interacting with the crustal structure of the African margin, in particular with the thick Pelagian continental lithosphere, the Malta Escarpment, and the Ionian oceanic lithosphere (Wortel and Spakman, 2000) (Figure 1). These three major tectonic domains, which originated during the Triassic period, were shaped by the fragmentation of the Pangea in the early Jurassic, leading to the opening of the Neo-Tethys Ocean (e.g., Stampfli *et al.*, 2002). Nowadays, the Calabrian subduction zone keeps moving south but at a much slower rate, suggesting that the whole system is subjected to opposing forces and/or that its driving mechanism, slab roll-back, is losing efficiency.

https://doi.org/10.5194/egusphere-2024-85
Preprint. Discussion started: 19 January 2024

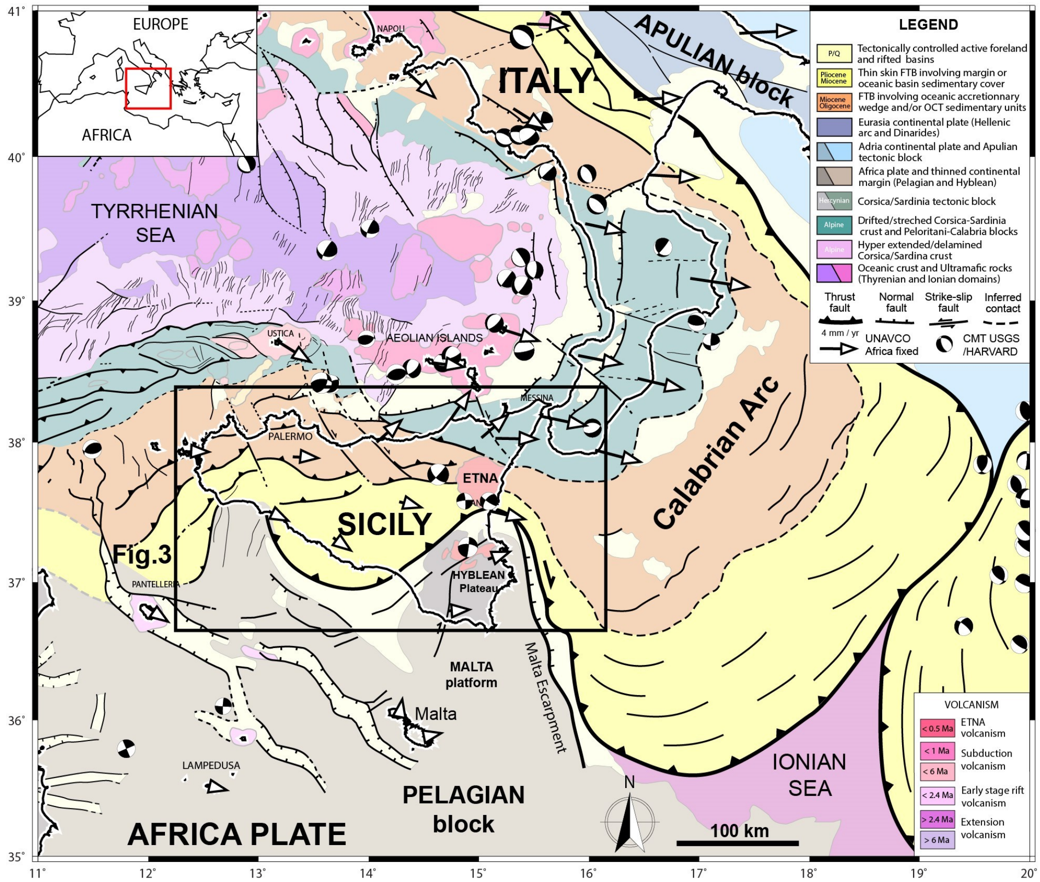

Figure 1: *Geodynamic and tectonic map of Central Mediterranean (modified from Henriquet et al., 2020). Geological data were synthetized from large-scale maps (e.g., Funiciello et al., 1981; Bigi et al., 1991; APAT, 2005; Lentini and Carbone, 2014). Structural data were synthetized from previous publications (e.g., Finetti et al., 2005; Chamot-Rooke et al., 2005; Corti et al., 2006; Prada et al., 2014; Lymer et al., 2018; Rabaute and Chamot-Rooke, 2019). Present-day Centroid Moment Tensors (Mw > 4.5) and GNSS data were retrieved from* https://www.globalcmt.org/CMTsearch.html *and* https://www.unavco.org/data/gps-gnss/gps-gnss.html *websites, respectively.*

Recent PS-InSAR satellite measurements (radar interferometry), published by Henriquet *et al.* (2022), have revealed an unexpected pattern of surface deformation across Southeastern Sicily, in particular, an eastward increasing subsidence of the whole Hyblean Plateau (Figure 2). This region has been partially investigated in previous studies, using similar techniques, but only captured local surface deformation features (Canova *et al.*, 2012; Vollrath *et al.*, 2017). Up to now, the origin of such a pattern of deformation remains,

https://doi.org/10.5194/egusphere-2024-85
Preprint. Discussion started: 19 January 2024

then, unexplained. Since satellite measurements were acquired over a very short period compared to typical seismic cycle durations (five versus several hundreds of years), and considering the discrepancy between satellite measurements and inferred long-term coastal uplift estimations (e.g., Bianca *et al.*, 1999; Ferranti *et al.*, 2006, 2010; Meschis *et al.*, 2020; Scicchitano *et al.*, 2008) (Figure 2a), we hypothesize that the satellite data are representative of the interseismic period. We further infer that the PS-InSAR data mainly document elastic loading mechanisms and reversible deformations. To explain the geodetic observations, we investigate the surface deformation signature of crustal and lithospheric deformation processes, including the impact of the southward migration of the Calabrian subduction system on the structural evolution of the eastern Hyblean margin as well as elastic loading and aseismic creep on coastal and offshore normal faults. We also test the potential surface expression of other processes such as volcanic deflation, hydrologic loading, and upwelling mantle flow.

2. Present-day deformation of SE Sicily

The kinematics and active tectonics in the SE Sicily are still a matter of debate, with major evolutions in the last decade (e.g., Argnani *et al.*, 2012; Bianca *et al.*, 1999), in particular with the acquisition of high-resolution bathymetry and seismic profiles in the adjacent Ionian domain (Dellong *et al.*, 2020; Gambino *et al.*, 2021, 2022; Gutscher *et al.*, 2016; Ridente *et al.*, 2014). Main reasons include the complex polyphased geological history of this region and the relatively low present-day horizontal strain rate (< 5 mm/yr), resulting from the slowdown of the Calabrian subduction zone activity in the last million years (Goes *et al.*, 2004).

2.1 Geodesy

https://doi.org/10.5194/egusphere-2024-85
Preprint. Discussion started: 19 January 2024

Geodetic surface measurements in SE Sicily include GNSS (e.g., Palano *et al.,* 2012), PS-InSAR/DInSAR (e.g., Vollrath *et al.,* 2017), and leveling datasets (e.g., Spampinato *et al.,* 2013).

PS-InSAR

In the present study, we use the first geodetic velocity field covering the whole Island of Sicily published by Henriquet *et al.* (2022) and derived from Sentinel-1 radar satellite (InSAR data) acquired during the 2015-2020 period. The PS-InSAR pseudo-3D velocity field (Up and E-W component) was obtained by merging ascending and descending acquisitions, combined with a reanalysis of the GNSS time series. Due to the acquisition geometry, Sentinel-1 radar satellite is not sensitive to the N-S component of horizontal surface deformation, which is, fortunately, very low in the studied region (Henriquet *et al.,* 2022). We therefore consider that, even if affected by minor distortions, the Up and E-W components of the pseudo-3D velocity data can be used with confidence (Supplementary Figures S2 to S5). The vertical (Up) component of this dataset reveals that the central and eastern parts of the Hyblean Plateau experience subsiding rates increasing eastward from 1 to nearly 3 mm/yr relative to the western coast (Figure 2). It should be noted that PS-InSAR data also show a slowly decreasing E-W component to the east of the Hyblean Plateau with velocities evolving from 3 to 2 mm/yr (fig.10, Henriquet *et al.,* 2022).

https://doi.org/10.5194/egusphere-2024-85
Preprint. Discussion started: 19 January 2024

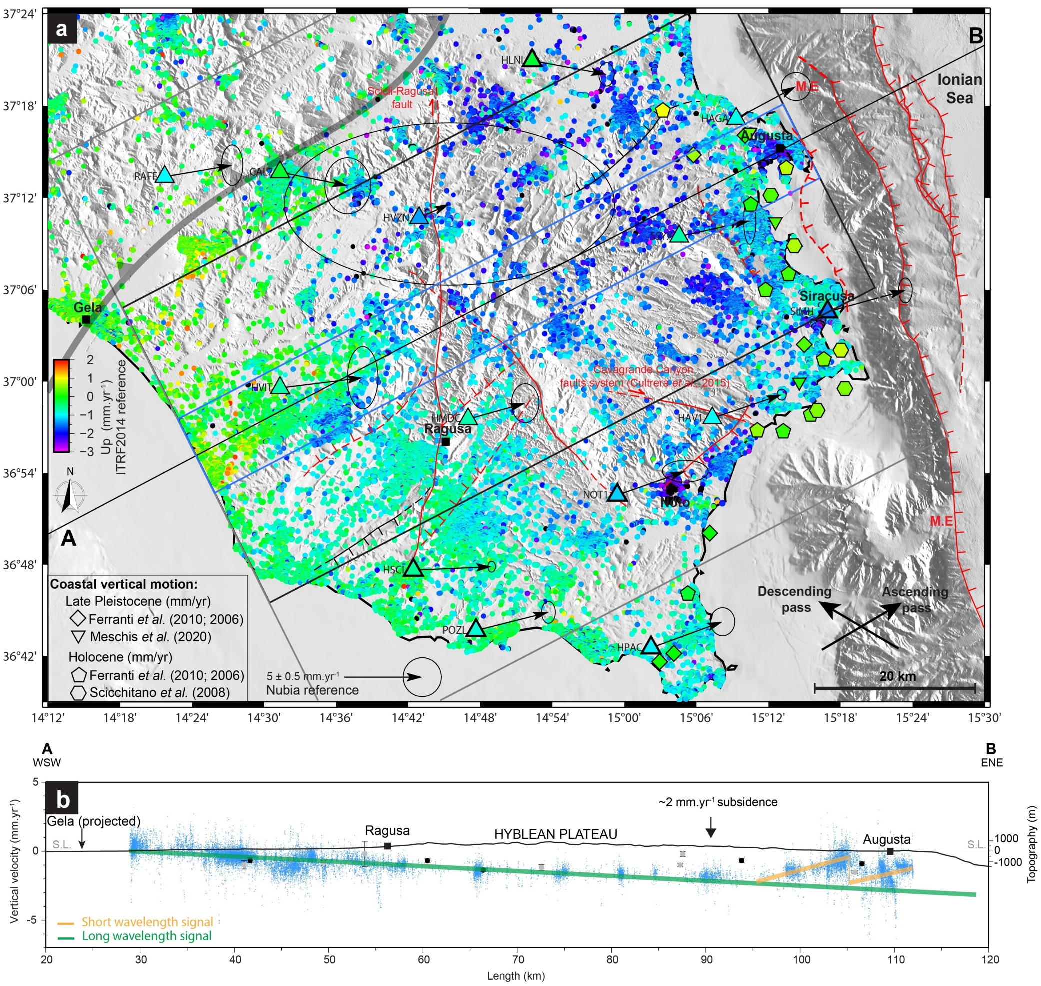

***Figure 2**: Geodetic data across the Hyblean Plateau region (see location in Figure 3). The Permanent-Scatterer (PS-InSAR) pseudo-3D Up velocities are from Henriquet et al. (2022) and are measured during the 2015-2020 period. GNSS 3D surface velocities are derived from a reanalysis of the Nevada Geodetic Laboratory (NGL) (Horizontal components reference: fixed Nubia; Up components reference: ITRF2014). Major faults of the Hyblean Plateau and Malta Escarpment (M.E) including the offshore normal faults identified by Gutscher et al. (2016) and analyzed by Gambino et al. (2021) (red: active fault; red dashed: inferred active fault; black: inferred aseismic slip (Spampinato et al., 2013)). SW-NE trending velocity profile showing surface velocity (Up) derived from PS-InSAR and GNSS stations vertical velocities. PS-InSAR data are stacked across a 5 km width on both sides of the AB profile (in blue). GNSS data are stacked using 20 km (in black) and 40 km (in gray) widths on both sides of the AB profile. Topographic and bathymetric profiles are presented without vertical exaggeration (V.E.x1).*

One should note that the zero reference of the PS-InSAR vertical velocity field is not precisely known. The vertical component of the pseudo-3D PS-InSAR velocity field and

https://doi.org/10.5194/egusphere-2024-85
Preprint. Discussion started: 19 January 2024

GNSS data have a ±0.5 mm/yr uncertainty in the ITRF2014 (Altamimi *et al.,* 2016), which implies that the observed subsidence over the Hyblean Plateau could be a little bit higher or slower. In the last case, slow uplift rates could be present in the Gela region. The vertical velocity trend is obtained by projecting and stacking the PS-InSAR data across a 5 km wide band along a N30°E AB profile (Figure 2b). Along this profile, oriented perpendicular to the main regional faults, the subsidence velocity reaches, in average, ~1 mm/yr between Gela and Ragusa and increases progressively to ~2.5 mm/yr between Ragusa and Augusta.

All along the eastern coast, a significant slower subsidence (or a relative uplift) is observed. From Augusta to Siracusa, and in the southernmost part of the Hyblean Plateau (HP), the subsidence rate decreases to about 1 mm/yr compared to the maximum subsidence rate in the central Hyblean Plateau (Figure 2). In the Gela region, PS-InSAR vertical velocities indicate a possible slow uplift rate of ~0.5 mm/yr (Figure 2). A second profile, located 20 km south of the AB profile shows the same eastward increase of the subsidence rates, evolving towards a similar relative uplift in the Siracusa region (Supplementary Figure S1).

Along the AB velocity profile, nor the Scicli-Ragusa inferred active fault (Vollrath *et al.*, 2017), nor the other major faults of the Hyblean Plateau can be evidenced in both the E-W and vertical components of the PS-InSAR data (Henriquet *et al.*, 2022) (Figure 2a), indicating that these faults are locked or are creeping at a slip rate lower than the PS-InSAR resolution (± 0.5 mm/yr). Locally, fast (> 3 mm/yr) subsiding zones, most probably related to human activities such as water pumping (Canova *et al.*, 2012), can be identified near the main cities of Augusta, Siracusa and Noto (Figure 2a).

Surface deformations signals extending over a hundred or more kilometers are most probably related to crustal or lithospheric scale processes (e.g., Stephenson *et al.*, 2022), whereas those extending over tens of kilometers are likely associated with much

https://doi.org/10.5194/egusphere-2024-85
Preprint. Discussion started: 19 January 2024

shallower and localized mechanical processes such as, seismic cycle deformation, volcanic bulging/collapse, hillslope instabilities (landslides), or human activities (water pumping, mining) (e.g., Vilardo *et al.*, 2009). We therefore hypothesize that the PS-InSAR vertical velocity field consists of two superimposed signals: (1) a long wavelength (> 100 km) subsidence, and gradual eastward tilt of the Hyblean Plateau (green line in Figure 2b), compatible with the decreasing PS-InSAR E-W velocities, and (2) a short wavelength signal, extending along the Eastern coast and characterized by sharp variations of the vertical velocities at kilometric scale (orange lines in Figure 2b).

GNSS

The Global Navigation Satellite System (GNSS) data used to calibrate the pseudo-3D PS-InSAR velocity field (Henriquet *et al.*, 2022) were based on the analysis of time series, retrieved from the Nevada Geodetic Laboratory (Blewitt *et al.,* 2018). We refine this analysis by correcting for annual and semiannual seasonal signals, instantaneous offsets, and gaps, using the time series inversion software developed by Masson *et al.* (2019). Across the Hyblean Plateau, GNSS velocities show horizontal velocities of ~2 mm/yr oriented homogeneously toward the ENE, in the Nubia reference frame (Figure 2). The vertical component of most of the GNSS stations shows an overall subsidence of the HP (-0.8 mm/yr in average) in the ITRF2014 reference frame (Altamimi *et al.,* 2016). This tendency is well illustrated by the high-quality NOT1 GNSS station located near the city of Noto, which has recorded the longest time series (23 years, 2000-2023), or by the SSYX and HMDC stations (Supplementary Figures S2 and S3). Overall, the GNSS vertical velocities are consistent with the median of the PS-InSAR vertical velocities calculated over an 8 km^2 region centered on each GNSS station (Supplementary Figures S2 to S5).

We used, then, this GNSS dataset to estimate a regional horizontal strain rate tensor, using the inversion model of Mazzotti *et al.,* 2005. The Hyblean Plateau is character-

https://doi.org/10.5194/egusphere-2024-85
Preprint. Discussion started: 19 January 2024

ized by an extension rate oriented SW-NE and a shortening rate oriented N165°E (Supplementary Figure S6), consistent with the focal mechanisms inversion (*Figure 3*).

2.2 Seismology

The instrumental seismicity map of SE Sicily, derived from INGV and Rovida *et al.* (2022) datasets (Figure 3), shows minor to moderate events (M<5) with deep crustal hypocenters (15-30 km). Over the Hyblean Plateau, earthquake hypocenters tend to roughly align along the inferred active, N-S trending, Scicli-Ragusa strike-slip fault (e.g., Vollrath *et al.,* 2017) and near the Cavagrande Canyon faults system (Cultrera *et al.*, 2015) (Figure 3). Most of these faults are probably inherited from the Plio-Quaternary tectono-magmatic phase of deformation (Henriquet *et al.,* 2019), and were partly re-activated in response to the ongoing Africa-Nubia/Eurasia plates convergence (e.g., Cultrera *et al.*, 2015; Mattia *et al.*, 2012). In this framework, the identification of the seismogenic source that triggered the 1693 event remains debated (e.g., Bianca *et al.,* 1999; Argnani and Bonazzi, 2005). The isoseists of Mw~7.4 Noto earthquake appear largely open toward the Malta Escarpment and Ionian Sea domains, suggesting the seismogenic faults could be located offshore (Figure 3). East of the Hyblean Plateau, earthquakes essentially distribute along the Malta Escarpment where a normal fault system, potentially responsible for the 1693 earthquake, has been identified (e.g., Bianca *et al.,* 1999; Gutscher *et al.,* 2016; Gambino *et al.,* 2021, 2022), (Figure 3).

The focal mechanisms over the Hyblean Plateau have dominant strike-slip characteristics, contrasting with the ~~extensive~~ deformation characterizing the NE corner of Sicily (Figure 3).

https://doi.org/10.5194/egusphere-2024-85
Preprint. Discussion started: 19 January 2024

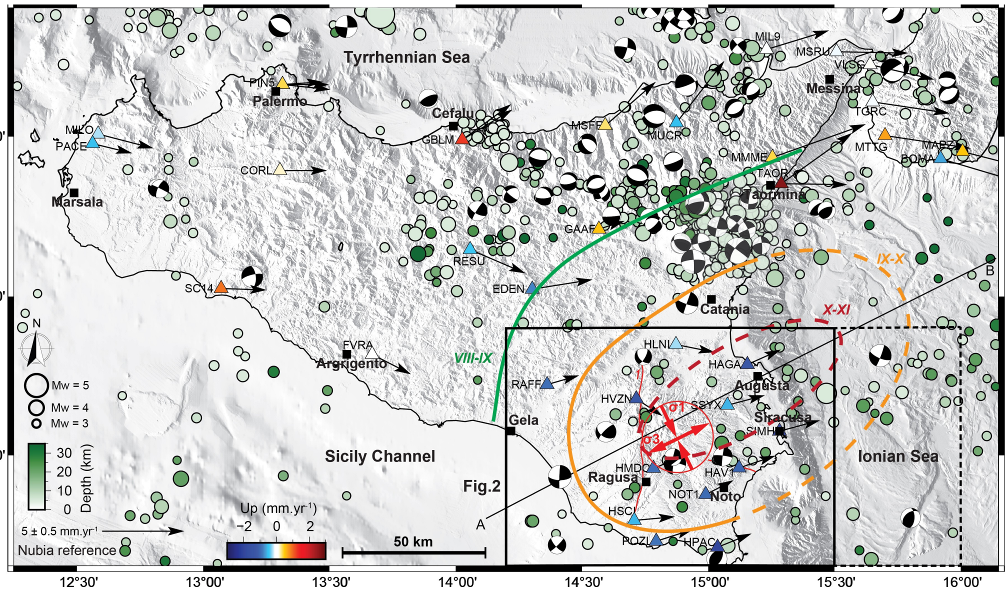

***Figure 3**: Instrumental seismicity of Sicily at crustal scale (0-30 km depth) showing earthquake hypocentral locations and focal mechanism solutions of M>3 events from 1985 to 2022 (Istituto Nazionale di Geofisica e Vulcanologia (INGV), 2005; Scognamiglio et al., 2006). 3D surface velocity derived from GNSS time series published in Henriquet et al. (2022) (Horizontal components reference: fixed Nubia; Up components reference: ITRF2014). Macroseismic intensity data of the 1693 Val-di-Noto Earthquake (M~7.4) from INGV CPTI15 database (Rovida et al., 2022): red dashed line = X-XI intensity, orange dashed line = IX-X intensity, green dashed line = VIII-IX intensity). Focal mechanisms stress inversion (red arrows) for the Hyblean Plateau region (black frame) and Ionian Sea (black dashed frame) using Michael's method (Vavryčuk, 2014; Levandowski et al., 2018). The AB profile shows the location of the PS-InSAR profile and synthetic structural cross-section presented in Figures 2 and 4.*

To estimate the present-day regional stress field across SE Sicily, we use the Vavryčuk's numerical model (Vavryčuk, 2014; Levandowski *et al.,* 2018), based on Michael's method (*Michael, 1984*). Results show that the regional stress across SE Sicily (Figure 3) is homogeneous (Supplementary Figures S7 and S8). The maximum compressive stress (σ_1) is horizontal and oriented N154°E ± 7°, compatible with the N160°E Africa-Eurasia plates convergence (e.g., Mattia *et al.*, 2012; Kreemer *et al.*, 2014). The minimum stress (σ_3) is oriented N64°E ± 7°, compatible with the GNSS extension rate (Figure 3).

https://doi.org/10.5194/egusphere-2024-85
Preprint. Discussion started: 19 January 2024

This regional stress field is compatible with the measured geodetic surface deformation (E-W extension) but does not explain the observed eastward-increasing subsidence rate across the HP.

2.3 Synthetic structural profile

To better constrain the deep structure and rheology of the studied area, we synthesize the available geological, and geophysical data into a 200 km long simplified crustal-scale structural cross-section following the N30°E AB profile crossing the Hyblean Platform, the Malta Escarpment, the western Ionian domain, and the offshore normal faults (Figures 2, 3 and 4). The eastern part of the synthetic structural profile is mainly based on seismic refraction profiles from Dellong *et al.* (2018), particularly the DY-P3 profile running sub-parallel to the AB profile and located 15 km further North, as well as seismic reflection profiles from Argnani *et al.* (2012), Gutscher *et al.* (2016), and Gambino *et al.* (2021, 2022) (Figure 4c). The structure of the western section is constrained by onshore and offshore geology, wells log stratigraphy, geophysics, seismic reflection profiles, and geological cross-sections from the ViDEPI project, Cavallaro *et al.* (2017), Scarfì *et al.* (2018), Henriquet *et al.* (2019) and Finetti *et al.* (2005).

https://doi.org/10.5194/egusphere-2024-85
Preprint. Discussion started: 19 January 2024

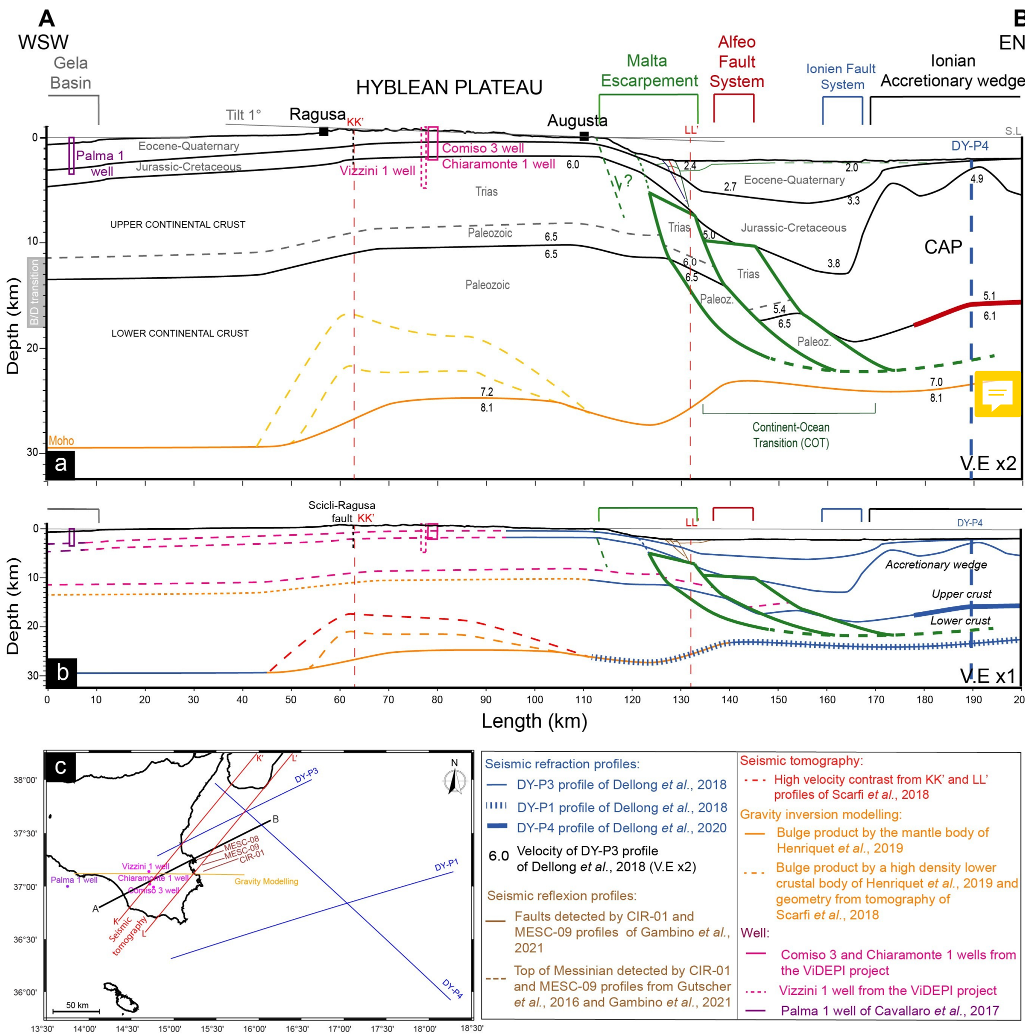

***Figure 4**: Simplified crustal cross-section along the N30°E AB profile (see Figures 4c and 2 for location). a) Two times vertically exaggerated synthetic structural profile along with seismic velocity data showing the structure and rheology of the Hyblean Plateau and eastern oceanic domain determined from onshore and offshore geology, wells stratigraphy, geophysics, seismic reflection, and refraction profiles (see Legend for references). Note the 1° tilt of the Hyblean Plateau topography toward the East. The red line corresponds to the inferred position of the main subduction décollement, and the green lines, refer to our interpretation of tilted blocks from the Malta Escarpment (M.E). b) Synthetic structural profile along available data (see Legend) without vertical exaggeration (V.E x1), showing the extent of the different datasets. c) Locations, in map view, of the AB profile, ViDEPI project wells data, tomography profile, refraction, and reflection seismic profiles.*

In the Hyblean domain, geophysical data (e.g., Sgroi *et al.*, 2012; Milano *et al.*, 2020) indicate that the crust has an average thickness of ~30 km. Based on gravity data

https://doi.org/10.5194/egusphere-2024-85
Preprint. Discussion started: 19 January 2024

modeling, Henriquet *et al.* (2019) ~~evidenced~~ a 100 km-large and 5 km-high lower crustal body below the Hyblean Plateau, locally uplifting the Moho to a depth of about 20-25 km. This feature is supported by tomographic data (Scarfì *et al.*, 2018). We constrain the geometry of the Quaternary to Mesozoic sedimentary cover of the Hyblean Platform and Gela basin using the Vizzini 1, Chiaramonte 1 and Comiso 3 wells (ViDEPI project) and the Palma 1 well (Cavallaro *et al.,* 2017).

In the DY-P3 seismic refraction profile (Dellong *et al.,* 2018), the 6.0 and 6.5 km/s velocity contours delimit two main steps deepening eastward at the junction between the Hyblean continental and Ionian oceanic domains (Figures 4a and 4b). Considering their locations along the Malta Escarpment that outlines the continent-ocean transition (COT), we interpret these velocity variations as deepening of the sediment/basement boundary, potentially related to tilted blocks of thinned continental crust formed during the Triassic-Early Jurassic rifting phase (see section 1) (e.g., Dellong *et al.*, 2018; Minelli and Faccenna, 2010; Scandone *et al.*, 1981; Tugend *et al.*, 2019).

As documented by Gutscher *et al.* (2016), and Gambino *et al.* (2021, 2022), the seismic reflection profiles (CIR-01, MESC-08 and MESC-09) shows several normal faults bounding and crossing the turbiditic valley, extending along the base of the Malta Escarpment (Gutscher *et al.,* 2016). This turbiditic valley fault system is constituted by three major parallel normal faults, 60 km long and dipping 35-50°E (Figures 4a and 4b), producing a strong morphological offset of the Ionian seafloor from the latitudes of Catania to Siracusa (cf. MESC-08 and MESC-09 seismic reflection profiles in Gambino *et al.,* 2021). We interpret these offshore normal faults as potentially related to recent re-activation of the shallow prolongation of the inferred Mesozoic tilted blocks (Figures 4a and 4b).

On the eastern side of the Hyblean domain, the Moho is constrained by DY-P3 and DY-P1 refraction profiles to a depth of ~30 km below the Malta Escarpment. To the east, in

https://doi.org/10.5194/egusphere-2024-85
Preprint. Discussion started: 19 January 2024

response to the bending of the Ionian slab, the Moho deepens northward from 20 km (DY-P1) to 32 km (DY-P3). Based on these data and the DY-P4 refraction profile (Dellong *et al.*, 2020), we estimate the depth of the Moho below the Ionian oceanic crust to be about 20-25 km in the eastern portion of the synthetic profile AB. In this region, the domain delimited by the seismic refraction velocities of 4.9-5.1 km/s has been interpreted as corresponding to the deformed sediments of the Calabrian accretionary prism (CAP) (Dellong *et al.,* 2018). Its thickness increases from 5 km (DY-P1) to 15 km (DY-P3), and it is evaluted to be ~11 km along the AB profile (Figures 4a and 4b). Note that the Calabrian backstop (i.e., Hercynian basement) is not present in the AB profile (Figures 4a and 4b). The location of the main subduction décollement along the AB profile has been estimated using the sharp velocity step (5.1-6.1 km/s) seismic refraction DY-P3 and DY-P4 profiles (Dellong *et al.,* 2018) at a depth of 15-20 km (red line in Figure 4a).

3. Mechanical model hypotheses

To explain the long wavelength bending trend evidenced by the PS-InSAR velocity Up component, we model the flexure of the Hyblean Plateau induced by (1) overloading of the continent-ocean transition (COT) domain in response to the SE migration of the very thick Calabrian accretionary prism (CAP), and (2) forced subsidence of the COT due to the local increase of the slab pull force imposed by the southward roll-back of the Ionian sub-duction. We hypothesize that these crustal/lithospheric deformation mechanisms may be strong enough to induce the large-scale subsidence and tilt evidenced by the geodetic data (PS-InSAR and GNSS) (Figure 2b). In addition, we test interseismic loading models on several onshore and offshore east-dipping normal faults, such as the Augusta-Siracusa fault, the Malta Escarpment, and the active faults documented by Gutscher *et al.* (2016) and Gambino *et al.* (2021, 2022), to explain the short wavelength deformation signal ex-tending along the eastern coast of the Hyblean Plateau (Figure 2b).

https://doi.org/10.5194/egusphere-2024-85
Preprint. Discussion started: 19 January 2024

3.1 Lithospheric flexure along a NNW-SSE profile

To better constrain key flexural parameters, such as the rigidity of the Hyblean and Ionian crust/lithospheres, the slab-pull force, and to investigate the impact of the Ionian slab roll-back, we first model the bending of the subducting Ionian slab along a NNW-SSE profile (CD profile), trending orthogonal to the AB profile (Figure 5a). As a structural reference, we use the isobaths of the top of the Ionian slab published by Hayes *et al.* (2018) (Figure 5a).

The lithosphere flexure models (as well as those in section 3.2) are calculated using the gFlex software (Wickert, 2016). We impose a no-displacement condition at the southern profile boundary and a broken plate with no bending moment and no shear at the northern boundary. The Ionian oceanic lithosphere is modeled assuming an effective elastic thickness (Te) ranging from 25 to 37 km (Figure 5b and Supplementary Figure S9), compatible with its Permo-Triassic age (e.g., Catalano *et al.,* 2001; Speranza *et al.,* 2012) and consistent with other publications (e.g., Watts and Zhong, 2000; Tesauro *et al.,* 2012; Cloetingh *et al.,* 2015).

The flexure of the subducting slab depends on its mechanical properties and on the loads induced by the sedimentary cover, the accretionary prism, and the slab pull force (Figure 5b). According to seismic refraction profiles DY-P1 and DY-P3 (Dellong *et al.*, 2018), the undeformed ante-Messinian sedimentary cover overlying the Ionian crust has a thickness of about 5 km. Thus, taking into account a depth of the Ionian Sea of 5-6 km, we consider that the top of the Ionian crust was lying at a uniform depth of 10-11 km before the onset of the Calabrian subduction system (Figure 5b). This depth corresponds to the isostatic equilibrium for the Ionian crust. It determines the initial geometry of the flexural model from which we calculate the bending induced by the Calabrian accretionary prism (CAP) load.

https://doi.org/10.5194/egusphere-2024-85
Preprint. Discussion started: 19 January 2024

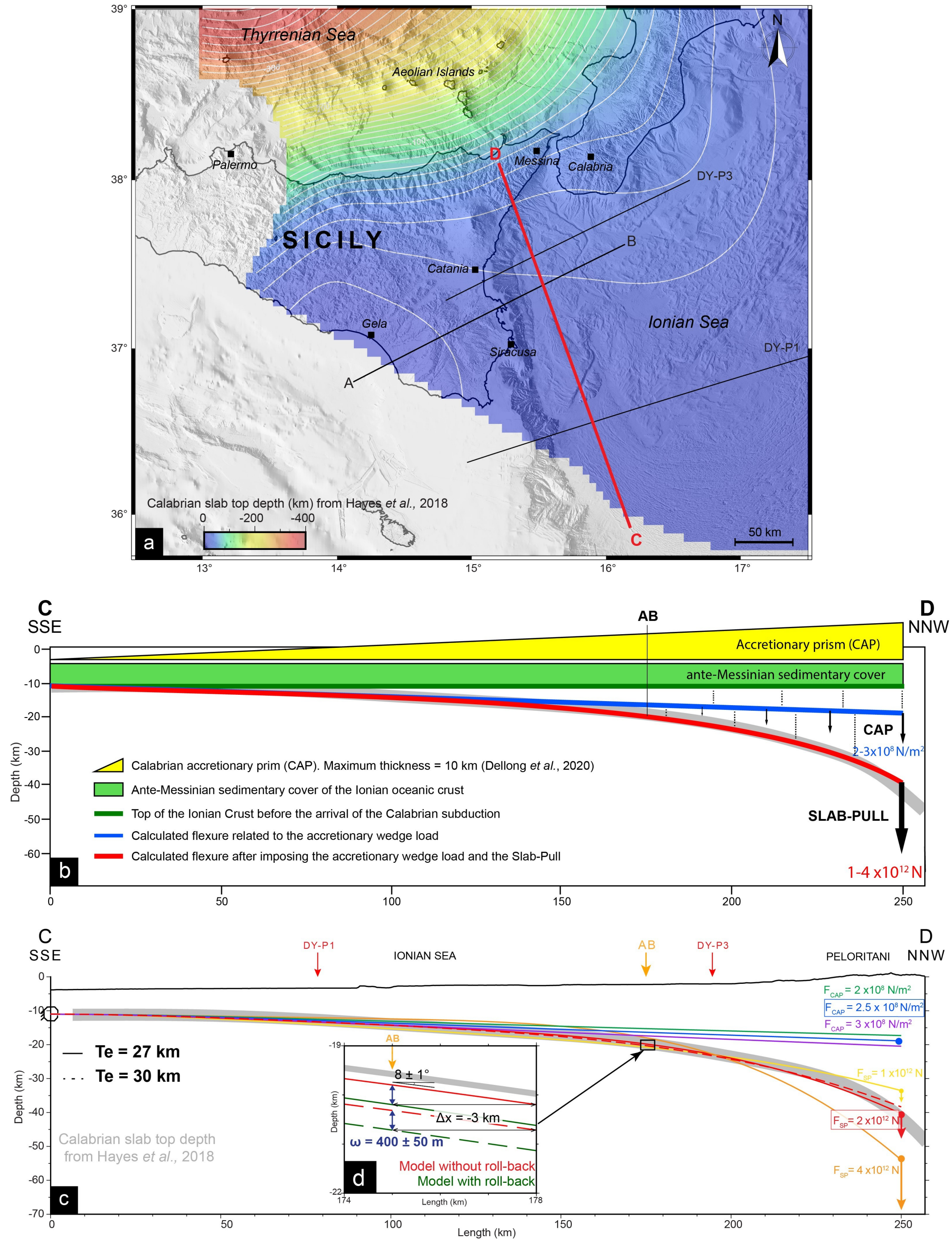

Figure 5: a) Map and isobaths of the top of the Ionian slab subducting below the Calabrian Arc (data extracted from Hayes et al., 2018). AB and CD profile locations are indicated, as well as seismic refraction profiles DY-P3 and DY-P1 (Dellong et al., 2018). b) NNW-SSE trending CD cross-section (in gray) showing the flat and steep ramp geometry of the Ionian slab (see location in Figure 5a) following the CD profile in a. The Ionian oceanic lithosphere supports a 5 km thick homogeneous ante-Messinian sedimentary cover (in

https://doi.org/10.5194/egusphere-2024-85
Preprint. Discussion started: 19 January 2024

green). The CAP thickness increases northward up to ~15 km (thickening of +10 km compared to the original 5 km thick undeformed sediment cover), according to Dellong et al. (2020) (in yellow), and the associated flexure is represented in a blue line. The bending of the slab is controlled by the slab pull, represented as a punctual load, ranging from 1-4 x10^{12} N, and added at the Ionian lithosphere flexure shown in a red line. c) The ante-Messinian cover and the CAP load are performed with a maximum CAP load of 2 x10^{8} N/m^{2} (green line), 2.5 x10^{8} N/m^{2} (blue line), or 3 x10^{8} N/m^{2} (purple line). Flexural models are performed with different effective elastic thicknesses (Te) ranging from 25 to 37 km (Supplementary Figure S9). We also consider elastic thicknesses of 25 and 30 km (Supplementary Figure S9) to perform the flexural model with different slab pull forces: 1 x10^{12} N (yellow line), 2 x10^{12} N (red line), and 4 x10^{12} N (orange line). Topographic, slab, and flexural model profiles are presented without vertical exaggeration (V.E.x1). d) Zoom of profiles CD and AB intersection where the depth difference between favorite models, a CAP load of 2.5 x10^{8} N/m^{2} and a slab pull of 2 x10^{12} N for an elastic thickness of 27 (continuous lines) and 30 (dashed line) km, without rollback (red line) and with rollback (green line), has been calculated. The local subsidence associated with the 3 km/Myr slab SE retreat is estimated to be about 400 ± 50 m.

Based on seismic refraction profiles DY-P4, DY-P1, and DY-P3 (Dellong *et al.,* 2018; 2020), the Calabrian accretionary prism thickness increases northward from 5 to 15 km. By removing the initial 5 km-thick Ionian sedimentary cover, the CAP load represents an increase in sediment thickness from 0 km at the southern end of the CD profile to 10 km at its the northern end. The Calabrian backstop, made of Hercynian continental crust, is not taken into account (Figure 5b).

The CAP load is calculated by:

$$F_{CAP} = \rho\, g\, h \qquad (1)$$

with a sediment density (ρ) of 2800 kg/m^{2} (profile 2D) according to Dellong *et al.* (2020), a gravity acceleration (g) of 9.81 m/s^{2}, and an increase of the CAP thicknesses (h) from 0 to 10 km.

The CAP load (F_{CAP}) is applied on the CD profile divided in 1-km-long segments by imposing a northward linear gradient from 0 to 2.75 x10^{8} N/m^{2} (equation 1) on the first 250 km of the profile (*Figures 5b and 5c*). We perform several tests with different maximum CAP load (F_{CAP}) and elastic thicknesses (Te) ranging from 2 x10^{8} to 3 x10^{8} N/m^{2} and 25 to 37 km, respectively. Models are tested with a constant mantle density of 3300 kg/m^{2} and no filling density for mantle restoration force (Figure 5c). The resulting flexure (~8 km maxi-

https://doi.org/10.5194/egusphere-2024-85
Preprint. Discussion started: 19 January 2024

mum), even if significant, is not sufficient to fit the Ionian slab profile (gray line in Figures 5b and 5c).

The slab pull force is then added to the northern termination of the Ionian lithosphere as a point load (Figure 5b). Flexural models are tested with different slab pull forces from 1 $x10^{12}$ to 4 $x10^{12}$ N, consistent with other publications reviewing slab rollback mechanical properties (e.g., Lallemand *et al.,* 2008), and the same range of elastic thicknesses from 25 to 37 km (Figure 5c and Supplementary Figure S9). The best fit to the Calabrian slab top is obtained for elastic thicknesses (Te) of 27-30 km, a maximum accretionary wedge load (F_{CAP}) of 2.5 $x10^{8}$ N/m^2, and a slab pull force (F_{SP}) of 2 $x10^{12}$ N (Figure 5c and Supplementary Figure S9). It's worth noting that including the CAP load significantly reduces the amplitude of the forebulge associated with slab bending, resulting in a flat-and-ramp geometry similar to that of the Ionian slab.

3.2 Crustal flexure along a WSW-ENE profile

The impact of the Ionian subduction roll-back on the deformation of the Hyblean Plateau is evaluated along the N30°E trending AB profile (Figure 5a), based on the following simplifications: (1) The ongoing roll-back induces incremental changes in the slab profile that corresponds to a southward translation and local deepening of the slab geometry. (2) This results in a local incremental increase of the accretionary prism thickness. (3) Due to the mechanical coupling of the Ionian slab and Hyblean lithosphere, the slab deepening exerts an incremental downward force on the COT (Figure 6).

The effective elastic thickness of the Hyblean lithosphere is less constrainable than that the Ionian lithosphere but should remain within standard values for a regular undeformed continental crust with an average geotherm. We test elastic thicknesses (Te) ranging from 25 to 40 km (Figure 6), assuming a uniform thickness, considering that the continent-ocean transition has the same elastic rigidity as the Hyblean crust and not taking into account the oceanic lithosphere.

https://doi.org/10.5194/egusphere-2024-85
Preprint. Discussion started: 19 January 2024

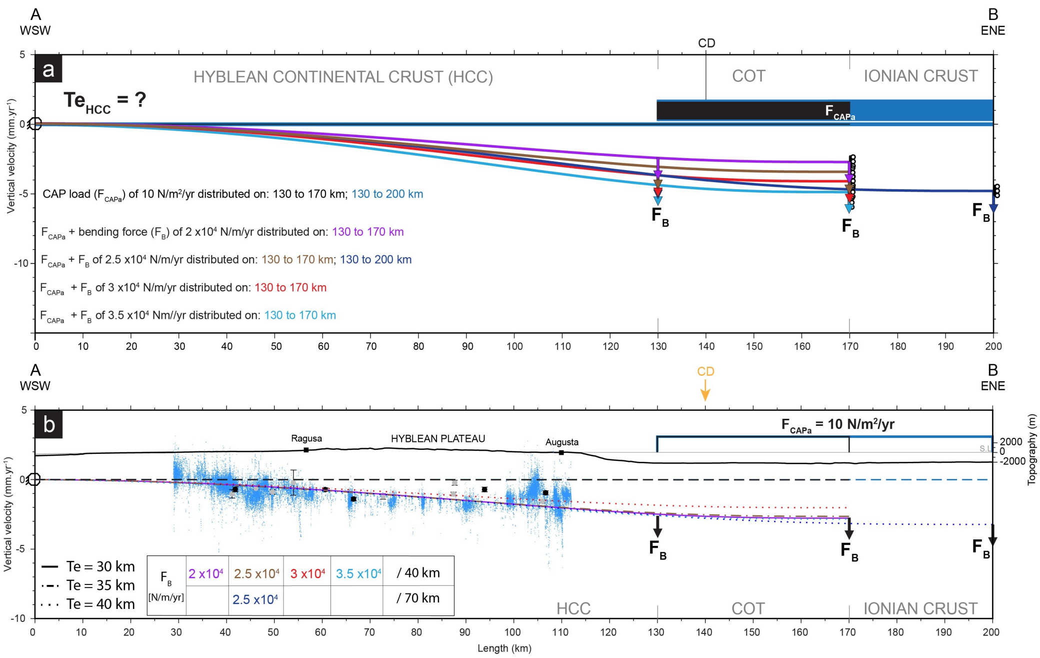

Figure 6*: a) Continental crustal flexure is controlled by the retreat of the Ionian slab along the AB profile. We calculated the flexure (gFlex from Wickert, 2016) induced by the only Calabrian accretionary prism load (F_{CAPa}) of 10 N/m²/yr distributed on 1-km-long segments on the ocean-continent transition (COT) (black line), and on the adjacent Ionian crust (blue line) from the 130 to 170 km and 130 to 200 km marks of the AB profile, respectively. We represent best models (Supplementary Figure S10) of the CAP load and a bending force (F_B) of 2 x10⁴ N/m/yr (purple line), 2.5 x10⁴ N/m/yr (brown line), 3 x10⁴ N/m/yr (red line), and 3.5 x10⁴ N/m/yr (light blue line) distributed on the COT, and of 2.5 x10⁴ N/m/yr (dark blue line) distributed on the COT plus into the Ionian crust. b) Best Hyblean crustal flexure models (Supplementary Figure S10) have elastic thicknesses of 30 km (continuous lines), 35 km (dotted-dashed lines), and 40 km (dotted lines). PS-InSAR velocities (in blue) and GNSS vertical velocities (NGL) with their uncertainties are stacked over 20 km (in black) and 40 km (in gray) along the AB profile (see location in Figure 2). Topographic and bathymetric profiles are presented without vertical exaggeration (V.E.x1).*

We first evaluate the flexural response due solely to the incremental increase of the CAP load induced by the southward migration of the slab profile, using our previous analysis of the bending of the Ionian slab. Based on the velocities of the GNSS stations situated in Calabria, we estimate the southward migration to 3 mm/yr, compared to a fixed Hyblean Plateau (Henriquet *et al.*, 2022). At the intersection between AB and CD profiles, at the 175 km length mark in the CD profile, the Ionian slab dips 8 ± 1° toward the north (Hayes *et al.*, 2018) (Figure 5d). Taking into account the CAP geometry, its southward motion, and the slab geometry, we calculate a local incremental thickening of the CAP of 4 $x10^{-4}$ m/yr (equivalent to 400 m/Myr) and a resulting load (F_{CAPa}) of about 10 N/m²/yr (Figure 5d). Ap-

https://doi.org/10.5194/egusphere-2024-85
Preprint. Discussion started: 19 January 2024

plying this load from the base of the Malta Escarpment to the eastern end of the Hyblean continental crust profile results in a very slow onshore subsidence rate of 5 x10^{-4} mm/yr maximum, 6000 time smaller than the PS-InSAR subsidence rate measured in the same area (~3 mm/yr).

We then investigate the effect of the southward Ionian slab roll-back and associated downward pull on the COT. We first calculate the flexural rigidity of the oceanic lithosphere (Turcotte and Schubert, 2014):

$$D=\frac{ETe^3}{12(1-\nu^2)} \qquad (2)$$

with a Young modulus (E) of 10^{11} Pa, a Poisson's ratio (v) of 0.25, and effective elastic thicknesses (Te) of 27-30 km (see 3.1). We obtain a flexural rigidity (D) of the Ionian lithosphere of 1.75-2.4 x10^{23} Pa.m^3.

To simulate the Ionian slab retreat, we translate the slab profile southward, assuming a slab retreat velocity of ~3 mm/yr (D'Agostino *et al.*, 2011) (Figure 5d). At the intersection of profiles AB and CD, this induces an incremental deepening of the Ionian slab of about 4 x10^{-4} m/yr (equivalent to 400 m/Myr), which defines the equivalent downward force at the same location along the CD flexure profile (Turcotte and Schubert, 2014):

$$F_B=\frac{\omega 2D}{x^2\left(L-\frac{x}{3}\right)} \qquad (3)$$

with an incremental deflection (ω) of 4 x10^{-4} m/yr (*Figure 5d*) and a flexural rigidity (D) of 1.75-2.4 x10^{23} Pa.m^3. The total profile length L corresponds to the point of the Hyblean lithosphere where the deflection (ω) is null, ~200 km based on the PS-InSAR and structural data (Figure 6). The distance x corresponds to the point where the deflection (ω) is estimated (intersection with profile CD). Considering L = 250 ± 50 km and x = 150 km, the equivalent incremental downward force is about 1-4 x10^4 N/m/yr.

This equivalent force (F_B) is then applied on the AB profile to model, with gFlex, the resulting flexure of the Hyblean crust/lithosphere. Flexural models are calculated with a no-displacement boundary condition at the southwestern end of the profile (20 km west of Gela) and a free displacement of a horizontally clamped boundary condition at its north-eastern end (80 km East of Malta Escarpment). Flexural models are run with a fill density of 2800 kg.m^{-3} solely for the CAP load. The downward force (F_B) and CAP load (F_{CAPa}) are homogenously distributed (on 1-km-long segments) over the 40 or 70 km long portion of the AB profile corresponding to the only continent-ocean transition (COT) or to the COT and adjacent Ionian crustal domain, respectively. We test different elastic thicknesses (Te) and bending force (F_B) ranging from 25 to 40 km and 1 x10^4 to 4 x10^4 N/m/yr, respectively (Figure 6b and Supplementary Figure S10).

To determine the best Hyblean crustal flexure models, we first filter the PS-InSAR vertical velocities (5 km stacked of the AB profile) using a 5 km width median filter with a step of 1 km. Comparing the resulting long-wavelength trend of the PS-InSAR data with the flexural models shows only misfits of less than 1 mm/yr. The comparison GNSS data (20 km stacked of the AB profile and 5 km large median filter with a step of 1 km) shows a higher misfit of less than 2.7 mm/yr due to a variable spatial density and quality of GNSS stations over the Hyblean Plateau (Supplementary Figure S10c). The best models (0.4 mm/yr RMS PS-InSAR) have elastic thicknesses of 30 to 40 km, a CAP load plus a bending force ranging from 2 x10^4 to 3.5 x10^4 N/m/yr distributed on the 40-70 km long portion of the AB profile (Figure 6b, and Supplementary Figures S10b, S10c). None of the tested continental crustal flexure models reproduce the short wavelength deformations observed

https://doi.org/10.5194/egusphere-2024-85
Preprint. Discussion started: 19 January 2024

in the Gela region (slow uplift of ~0.5 mm/yr) or along the Augusta-Siracusa coastal area (slower subsidence of -1 mm/yr).

3.3 Interseismic loading and aseismic creep on coastal and off-shore faults

Along the coast, from Augusta to Siracusa, PS-InSAR vertical velocities vary at a kilometer scale, and appear 1-3 mm/yr slower than the general trend of subsidence affecting the Eastern Hyblean Plateau (Figures 2a and 6b). Interestingly, these short wavelength signals show triangular patterns similar to those produced by shallow faulting in an elastic domain. To investigate the sources of these surface deformation, we test several scenarios involving interseismic loading and aseismic creep on coastal and offshore faults.

Offshore, several active normal faults, outcropping at the base of the Malta Escarpment, have been imaged by Gutscher *et al.* (2016) and documented in detail by Gambino *et al.* (2021, 2022). Along the coastline, the Augusta-Siracusa fault (Figure 7) has been also considered as a potential active fault (e.g., Azzaro and Barbano, 2000; Bianca *et al.*, 1999). We use the Coulomb 3.4 software (Toda *et al.*, 2011) to impose different fault slip rates and geometric boundary conditions on these fault systems, assuming standard elastic properties (Poisson's ratio of 0.25, Young modulus of 80 GPa).

The model predictions are compared to the PS-InSAR short wave-length signals (Figure 7b) obtained by removing the mean of best fitting flexural models (see section 3.2) from the original geodetic dataset. Two patterns of relative uplifts of about 2.5 ± 0.5 mm/yr, gently tapering westward, can be identified near and to the SE of Augusta with a zone of relative subsidence of about -2 ± 1 mm/yr in between them (Figure 7a). We hypothesized that these surface deformations could be induced by fault slip along ENE-dipping normal fault systems (Figure 7).

https://doi.org/10.5194/egusphere-2024-85
Preprint. Discussion started: 19 January 2024

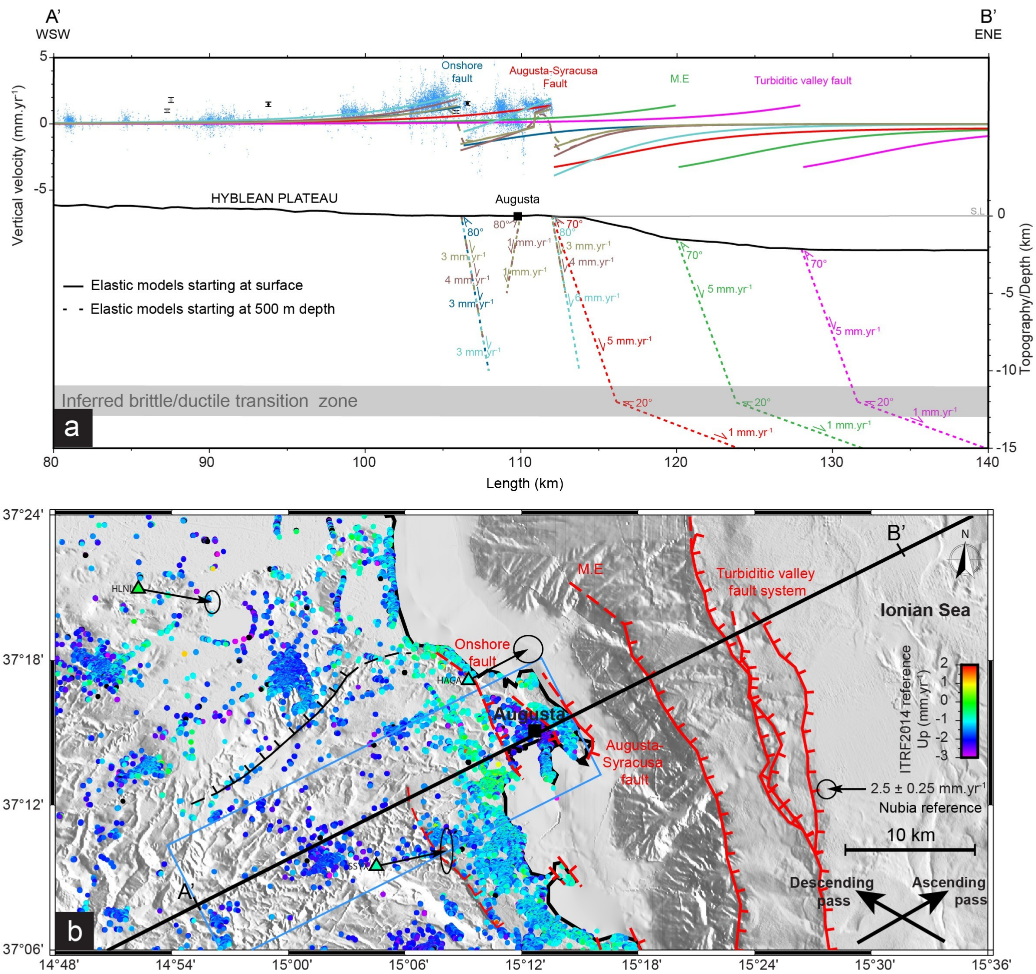

Figure 7: a) Coulomb 3.4 (Toda et al., 2011) numerical models of interseismic elastic loading (step of 100 m) on offshore and coastal inferred active faults along the eastern Hyblean Platform. PS-InSAR Up velocities are stacked across a 5 km width on both sides of the AB profile and appear in blue. Modeled interseismic deformations related to: the turbiditic valley normal fault identified by Gutscher et al. (2016) (magenta line); the Malta Escarpment (green line); the Augusta-Siracusa coastal fault (red line); onshore inferred active faults in Augusta (dark blue line). Modeled elastic loading of the Augusta-Siracusa coastal fault plus onshore inferred active faults in Augusta are represented in light blue, light, and dark brown lines. Topography/depth is represented without vertical exaggeration (V.E.x1). b) Map view of geodetic data in the northeastern part of the Hyblean Plateau. Major faults of the Hyblean Plateau including the Augusta-Siracusa coastal fault and the inferred onshore active fault, and Malta Escarpment (M.E) including the turbiditic valley faults identified by Gutscher et al. (2016) and analyzed by Gambino et al. (2021, 2022) (red: active fault; red dashed: inferred active fault; black: inferred aseismic slip (Spampinato et al., 2013).

A first set of models corresponds to interseismic locking of the shallow (0 to 10-15 km depth) sections of the main normal faults identified in the study area (Figure 7b), and elastic loading by deep (> 15 km depth) creeping sections. Regardless of the deep fault geometry or slip rates, all these models generate generalized long-wavelength subsidence

https://doi.org/10.5194/egusphere-2024-85
Preprint. Discussion started: 19 January 2024

rates, incompatible with the geodetic data (green dotted line, Supplementary Figure S11). Thus, we dismiss interseismic loading as a potential mechanisms to explain the short wavelength uplift-subsidence patterns.

The second set of models correspond to shallow aseismic slip on three offshore normal faults: the Augusta-Siracusa coastal fault (Bianca *et al.*, 1999), the Malta Escarpment, and the turbiditic valley fault (Gutscher *et al.,* 2016; Gambino *et al.,* 2021, 2022) (Figure 7a and Supplementary Figure S11). The modeled faults (Figure 7a) share a similar listric geometry with a first fault plane dipping 70°NE and extending from the surface to 12 km depth (inferred brittle/ductile transition zone), and a second one dipping 20°NE and extending from 12 to 50 km depth (to limit boundary effects). We imposed slip rates of 5 mm/yr on the first fault plane, based on Meschis *et al.* (2020) model (Supplementary Figure S10), and 1 mm/yr on the second plane to dampen the elastic deformation produced by slip on the shallow fault (Figure 7a). Aseismic slip on these various faults produces coastal uplift rates, reaching at most ~1 mm/yr for the Augusta-Siracusa fault, consistent with the PS-InSAR measurements east of Augusta (*Figure 7a*). However, all the modeled offshore faults failed to reproduce the ~2-3 mm/yr uplift rates measured west of Augusta (Figures 7a and 7b).

The third set of models focus on surface deformation generated by aseismic creep on 70-80° ENE-dipping shallow fault planes. We first simulate slip on the upper portion of the Augusta-Siracusa fault but ~~it~~ this model succeed in producing sufficient uplift east of Augusta it failed to reproduce the observed relative uplift west of Augusta. Based on PS-InSAR data, and structural evidences of onshore normal faulting (Gambino *et al.,* 2021), we added to the previous Augusta-Siracusa fault model a 80° dipping onshore normal fault outcropping at the 106 km mark of the AB profile, with a slip rate of 3 mm/yr down to 10 km depth (light blue lines in Figure 7a). The surface deformation generated by this dual creeping fault can explain the observed PS-InSAR relative uplift between the 103 and 106 km

https://doi.org/10.5194/egusphere-2024-85
Preprint. Discussion started: 19 January 2024

profile marks and 110 and 112 km. Imposing aseismic slip on the onshore normal fault alone fails to reproduce the subsidence east of Augusta (dark blue line in Figure 7a).

The triangular patterns of sharp steps and associated lows in the PS-InSAR data could be also fitted by a model involving shallower aseismic creep (up to 5 to 8 km depth) and combining the onshore ENE-dipping fault (106 km mark), creeping at 3-4 mm/yr, an antithetic onshore WSW-dipping fault (110 km mark), creeping at 1 mm/yr, and the Augusta-Siracusa coastal fault (112 km mark), creeping at 3-4 mm/yr (brown lines in Figure 7a). This ad-hoc model illustrates that the short wavelength geodetic signal along the Eastern Hyblean Plateau coast can be explained with ongoing extension tectonics and creep on coastal normal faults. We test the same configuration (two onshore faults and the Augusta-Siracusa coastal fault) with a fault plane propagating to the surface up to 500 m depth (Figure 7a). This model, equivalent to a blind fault, induces vertical surface deformation (between the 106 and 110 km marks) about 0.2 mm/yr slower than the model starting to creep from the surface, but still remains consistent with the PS-InSAR data.

3.4 Alternative hypothesis

To explore others hypothesis that could explain part of the obeserved geodetic velocity patterns, we explore three alternative models:

Mantle flow upwelling

Seismic tomography and volcanic data identify a slab window extending along most of the northern coast of Sicily, with a slab break-off recently propagating from west to east and potentially triggering toroidal and upwelling mantle flows (Civello and Margheriti, 2004; Faccenna, 2005; Scarfì *et al.*, 2018; Trua *et al.*, 2003). This process could induce long wavelength surface motions (so-called dynamic topography) over the whole Sicily. However, numerical models of the mantle flow mainly predict areas of uplift and subsidence restricted to Mount Etna and the southern Peloritani region (Faccenna *et al.,* 2011; Gallen *et*

https://doi.org/10.5194/egusphere-2024-85
Preprint. Discussion started: 19 January 2024

al., 2023). Thus, SE Sicily appears to be situated too far from the Ionian slab edge to be affected by upwelling mantle flow. It is therefore unlikely that hypothesis explains the observed vertical surface deformation.

Volcanic deflation

The most recent major volcanic activity documented on the Hyblean Plateau dates back 1.4 Myr (Schmincke *et al.,* 1997; Behncke, 2004), but recent minor volcanic activity, not recorded at the surface, cannot be totally ruled out. In such a case, volcanic material deflation located below the central Hyblean Plateau could induce local subsidence rates affecting a large region. We tested this hypothesis numerically with deflating spheres (Mogi model, Supplementary Figure S12) situated at a depth of 8 km, at the top of the Paleozoic basement and possible location of magma accumulation (Henriquet *et al.,* 2019). Our first-order tests show that even using extreme deflations of 50-75%, the PS-InSAR subsidence rates cannot be reproduced (Supplementary Figure S12), rendering the volcanic deflation hypothesis extremely unlikely.

Hydrologic loading

The geology of the Hyblean Platform is mainly composed of limestones and dolomites in a karstic environment. Long-term recharge or discharge of karst aquifers is known to induce transient elastic deformation, measurable with geodetic data (e.g., D'Agostino *et al.,* 2018; Silverii *et al.,* 2016; Grillo *et al.,* 2011). Testing this hypothesis on the Hyblean Plateau would require data and modeling of the vegetation cover, farming activity, bulk volume, soil absorption capacity, etc., which is beyond the scope of the present study. A detailed analysis of GNSS data could uncover such a hydrological signal, unfortunately, the Hyblean Plateau only comprises 14 GNSS stations, of variable qualities. The best-quality stations, NOT1 and HSCI show minimal pluri-annual signals potentially associated with hydrological variations (Supplementary Figures S2 and S4), which cannot ex-

https://doi.org/10.5194/egusphere-2024-85
Preprint. Discussion started: 19 January 2024

plain the long wavelength trend observed over the Hyblean Plateau. Hydrologic loading, as a source of large scale surface subsidence, is then unproved.

4. Discussions

4.1 Short-term and long-term model limits

We explain the eastward tilt and subsidence rates of the Hyblean Plateau as the flexure of the Hyblean continental crust/lithosphere induced by the southward migration of the Calabrian accretionnary prism (CAP) and retreat of the Ionian subducting slab (sections 3.1 and 3.2). This model is based on the assumption that the geodetic data (GNSS and PS-InSAR) measured over a short-period (5-15 years) are representative of the kinematic evolution of the studied region at the scale of a few thousand years. Flexural modeling indicated that the increasing loading of the COT, induced by the southward propagation of the CAP, is not sufficient (Figure 6b). The increase in bending force, imposed by a ~3 mm/yr southward retreat of the Ionian slab, gives interesting positive results. This process could be strong enough to pull-down the Eastern termination of the Hyblean crust at velocities compatible with PS-InSAR measurements. However, we obtained this result considering that the Hyblean crust/lithosphere, the continent-ocean transition (COT), and the Ionian crust/lithosphere have similar mechanical properties. This assumption implies that the COT has a significantly rigid, and potentially too strong rheology (Figure 8) as discussed hereafter (section 4.2).

We used simple 2D elastic model based on parameters determined through analytical modeling of the Ionian oceanic lithosphere flexure using, as a reference, the Ionian slab geometry determined by Hayes *et al.* (2018). The use of more advanced numerical models (FEM), including 3D modeling methods would likely improve our first-order estimates. Similarly, the lateral variations of the Hyblean continental crust thickness and elas-

https://doi.org/10.5194/egusphere-2024-85
Preprint. Discussion started: 19 January 2024

tic properties are not accurately known. We used the available geophysical data (Henriquet *et al.*, 2019; Scarfì *et al.*, 2018), but it was not possible to constrain the Hyblean crust/lithosphere rheology with a better confidence (Figure 8). Should such parameters become available in the future, they could be used to refine our Hyblean crust/lithosphere flexure calculations.

One of the other assumptions we made concerns the rate of increase in the slab bending force due to the southward propagation of the Ionian slab roll-back. The calculated increase in slab bending force east of the HP is based on the estimated rate of southward retreat of the Ionian slab defined by the mean of the GNSS NS horizontal velocities in southwest Calabria (using as a reference the Malta Island). However, this estimation may be underestimated if the Calabrian Arc migrates southward slower than the Ionian slab, due to its mechanical interactions with the Apulian and African margins.

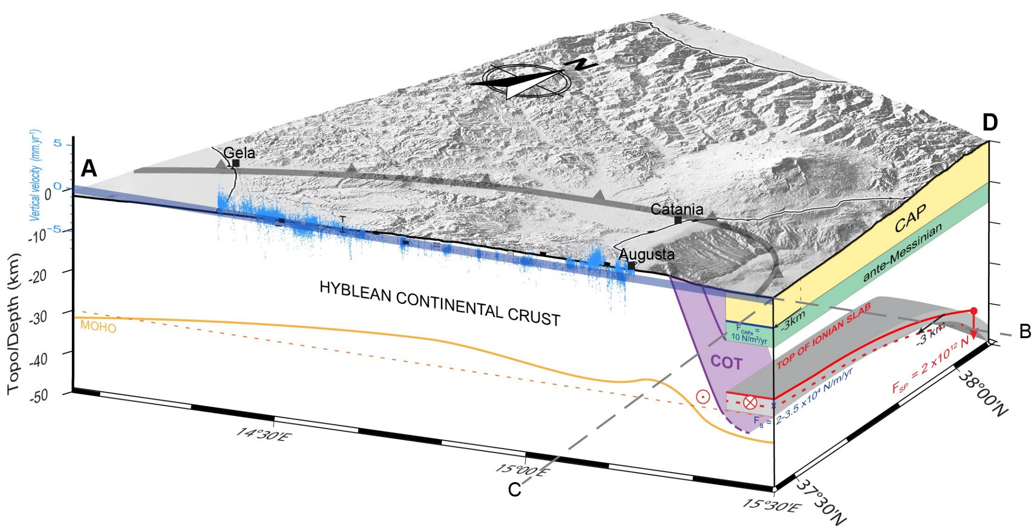

Figure 8: *Schematic 3D deformation model of Southeastern Sicily controlled by Ionian slab roll-back delimited by profiles AB and CD. The 3 km southward retreat of the Ionian crust flexure model (red dashed line) is not at scale. The Moho of the Hyblean continental crust determined by geophysical data (Henriquet et al., 2019; Scarfì et al., 2018) is shown in orange. The dashed orange line represents the averaged Moho depth used for flexural modeling calculations. The continent-ocean transition (COT) is shown in purple, and the Calabrian accretionary prism (CAP) is shown in yellow.*

https://doi.org/10.5194/egusphere-2024-85
Preprint. Discussion started: 19 January 2024

The short-wavelength relative uplift signal, observed in the geodetic data along the Southeastern Sicily coast, must be driven by more shallow deformation mechanisms than those responsible for the long-wavelength eastward flexure of the HP (Figure 6b). Kilometer long surface deformations are typically related to upper crustal deformation processes (e.g., Burgmann and Thatcher, 2013), so we test interseismic loading models on the inferred and identified onshore and offshore fault systems.

Slip on the Malta Escarpment and turbiditic valley normal fault (Gutscher *et al.*, 2016; Gambino *et al.*, 2021, 2022) cannot explain the observed deformation of the eastern coast of the Hyblean Plateau. Only creep on the Augusta-Siracusa coastal fault and the antithetic structure (Bianca *et al.,* 1999; Azzaro and Barbano, 2000) induce onshore vertical deformation compatible with the geodetic data near Augusta. Interseismic slip (creep) on two onshore ENE and WSW 80°-dipping faults, and the Augusta-Siracusa coastal fault fits with the PS-InSAR data in the Eastern of the AB profile. These faults could be associated to a Triassic NW-SE graben/horst structure, the Augusta Graben, extending from Augusta to Siracusa (e.g., Grasso and Lentini, 1982).

Our results suggest that these faults should creep up to the surface or the near-surface (blind fault) to produce sufficient interseismic surface deformation in the footwall. In that latter case, their surface expression could correspond to gentle surface folding or to fold scarp morphologies (e.g., Chen *et al.*, 2007; Li *et al.*, 2015) rather than localized cumulated fault scarps.

High precision leveling data acquired between 1970-1991 and analyzed by Spampinato *et al.* (2013), reveals a remarkable ~4 mm/yr velocity offset between benchmarks 107 and 113, both situated near the coast 5 km west of Augusta (Figure 9c). This sharp vertical velocity gradient is correlated with a marked topographic step, trending NS, and descending toward the sea. Northwest of Augusta, the leveling dataset also shows a ~2

https://doi.org/10.5194/egusphere-2024-85
Preprint. Discussion started: 19 January 2024

mm/yr offset between benchmarks 119 and 120, associated to a topographic step, oriented E-W, and facing north (Figures 9b and 9c).

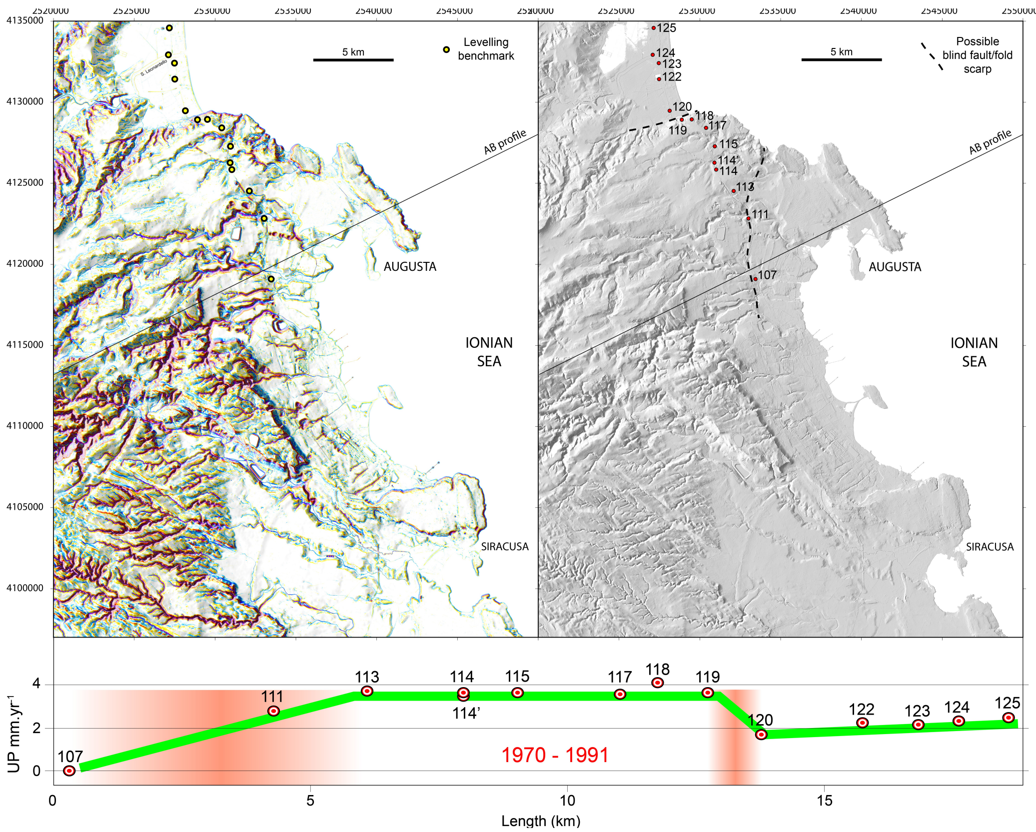

Figure 9: *1970-1991 leveling profile from Spampinato et al. (2013) performed along the Siracusa-Augusta coastal domain. a) Morpho-structural map of the Augusta-Siracusa region showing fluvial incision networks and morphological scarps. The location of leveling benchmarks appears in yellow circles. b) Shaded DEM showing the location of leveling benchmarks with their reference numbers and potential tectonic fault/fold scarps. c) 1970-1991 leveling profile showing a first velocity step (~4 mm/yr) between benchmark 107 and 113, and a second one (~2 mm/yr), between benchmark 119 and 120 (potential fault zone locations appear in the background in red).*

A morpho-structural analysis of this area, using a 5 m resolution DEM, outlines potential drainage incision anomalies, oriented perpendicular to the identified topographic steps, potentially related to tectonic surface uplift (Figure 9c). The topographic step between benchmarks 119 and 120 (Figures 9a and 9b) could correspond to the Scordia-Lentini Graben border (e.g., Cultrera *et al.*, 2015). The topographic anomaly between benchmarks 113 and 107 and extending to the north up to the Ionian Sea, and to the

https://doi.org/10.5194/egusphere-2024-85
Preprint. Discussion started: 19 January 2024

South toward Siracusa, was not previously identified as a tectonic feature. It could correspond to the implemented creeping fault, used to match the PS-InSAR data. Uplifted late Quaternary marine terraces have been evidenced in this region (Bianca *et al.*, 1999; Meschis *et al.*, 2020; Monaco and Tortorici, 2000), but the authors didn't mention a tectonic origin for the measured coastal uplift. Finally, the measured fast uplift velocity (3-4 mm/yr) could be considered as inconsistent with the low amplitude of the topographic scarp measurable in the field (a few tens of meters). This point is discussed hereafter (section 4.2).

4.2 Combined long-term tectonics and seismic cycle model

The subsidence and tilt patterns observed in the geodetic data can be explained by the combination of (1) the flexure of the Hyblean continental crust induced by the bending force associated to the Ionian subduction roll-back and the CAP overload, explaining the long-wavelength deformation affecting the HP, and (2) the aseismic activity on the Augusta-Siracusa fault and offshore fault bordering the eastern coast of the Hyblean Plateau, explaining the short-wavelength deformation signal affecting the Augusta/Siracusa region (Figure 10). In this section, we discuss how this short-term (geodetic) model can be combined with long-term geological and tectonic observations.

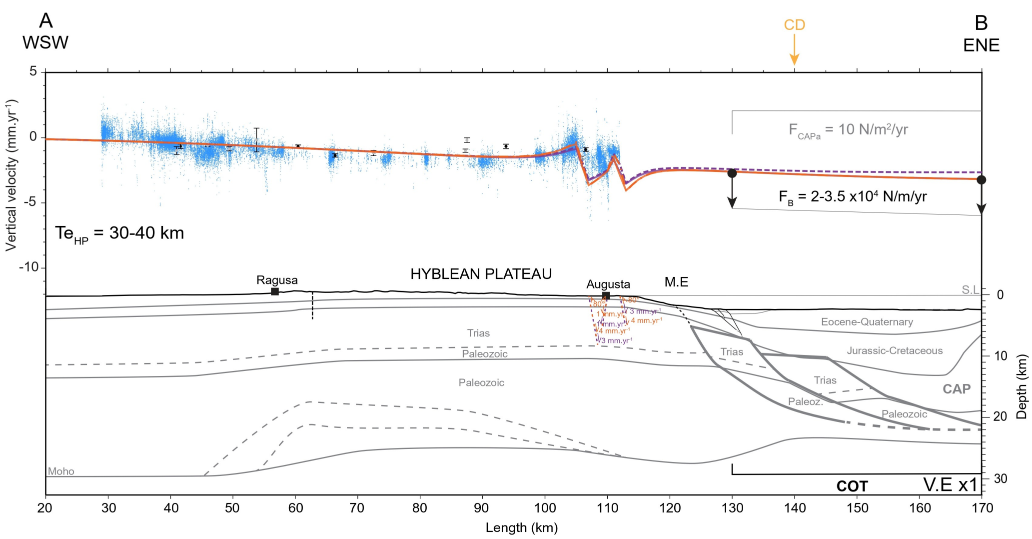

https://doi.org/10.5194/egusphere-2024-85
Preprint. Discussion started: 19 January 2024

***Figure 10 :** The final model combining the possible range of the Hyblean continental crust flexural models and the surface deformation (step of 1 km) induced by fault creep (from surface, continuous lines) or active folding in the Augusta-Siracusa coastal domain (from 500 m, dashed lines). In this model, the flexure of the Hyblean continental crust is essentially controlled by the bending force associated with the Ionian slab roll-back and, to a lesser extent, by the Calabrian accretionary prism load (CAP). The synthetic structural profile (gray) and topography have no vertical exaggeration (V.E.x1).*

Initial geological analyses suggest that the eastern coast of SE Sicily has been relatively stable over the last million year, with maximal subsidence and uplift amplitudes of ±0.2 mm/yr (Ferranti *et al.,* 2006). More recently, dating of Late Quaternary marine terraces along the Siracusa-Augusta coastal domain indicates that the eastern coast of the Hyblean Plateau has experienced a slow constant uplift during the last 500 Kyr, increasing northward from 0.1 to 0.4 mm/yr (Meschis *et al*., 2020). On a shorter historical time scale based on Roman archaeological site studies, Scicchitano *et al.* (2008), propose that the Siracusa coast has been slowly uplifting during the last 4 Kyr, albeit with significant uncertainties. These long-term observations, extending from the Quaternary to historical time, point to a slow regional uplift, apparently in contradiction with the geodetic data. Interestingly, along the N30°E trending AB synthetic profile, a ~1° generalized eastward tilting of the HP topography can be evidenced (Figure 4a). The origin of this tilt, in apparent agreement with the geodetic data, could be rather related to the Plio-Quaternary formation of the HP (Henriquet *et al*., 2019). To reconcile long and short time scale surface motions, we propose an original seismic cycle model, driven by the southward roll-back of the Ionian subduction (Figure 11).

https://doi.org/10.5194/egusphere-2024-85
Preprint. Discussion started: 19 January 2024

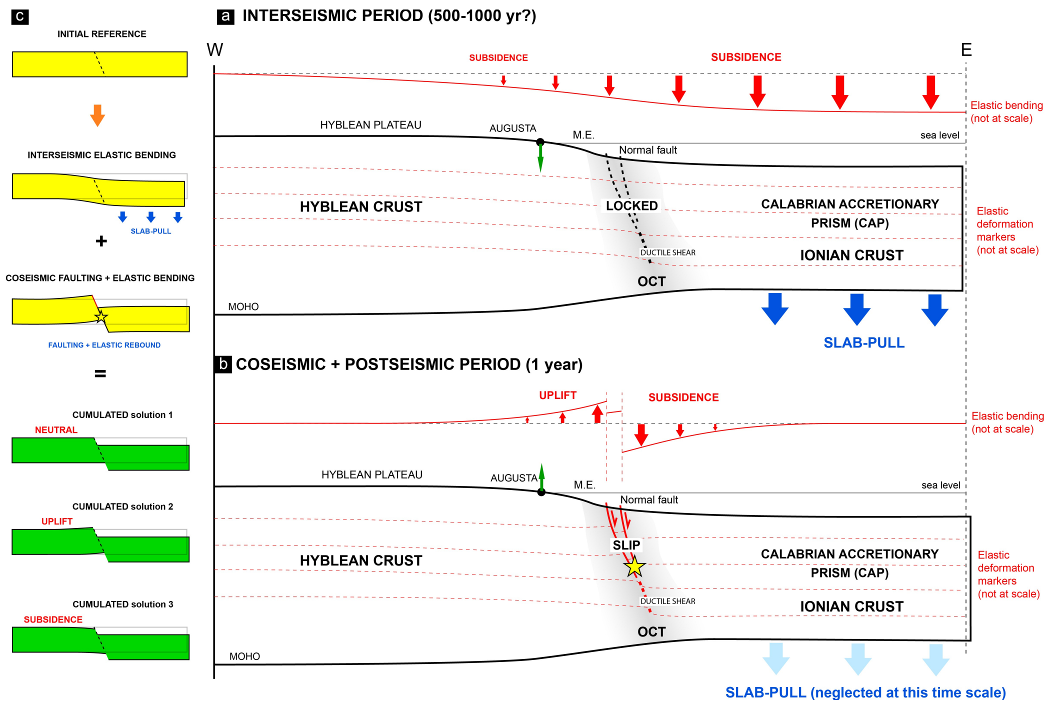

Figure 11: Schematic model of seismic cycle for south-eastern Sicily, integrating crustal elastic bending, aseismic, and seismic faulting controlled by slab-pull. a) Interseismic period, b) coseismic and postseismic period, c) different scenarios of the cumulated interseismic, postseismic, and coseismic. This model could reconcile short and long-term observations.

During the interseismic phase, the active onshore and offshore normal faults affecting the eastern HP are locked. The Hyblean and Ionian crusts are coupled and can be compared to an elastic beam, bending eastward in response to an increasing downward vertical force: the slab pull induced by the Ionian slab roll-back (Figure 11a). Considering a minimum 500 yr return period for earthquakes such as the 1693 Val-di-Noto event (Bianca *et al.*, 1999; Meschis *et al.*, 2020), and extrapolating the PS-InSAR measurements on that period, coastal subsidence along the Siracusa-Augusta region could reach 1-2 m. This subsidence could be significantly reduced if the onshore faults, potentially related to extrados deformation, creep aseismically during that period. During the coseismic and postseismic phases, the Malta Escarpment fault unlocks, and seismic slip induces (for a Mw>7

https://doi.org/10.5194/egusphere-2024-85
Preprint. Discussion started: 19 January 2024

earthquake) multi-metric subsidence of the hanging wall and an associated decametric to metric uplift of the foot-wall (e.g., Wells and Coppersmith, 1994) (Figure 11b).

The cumulated succession of inter-seismic coastal subsidence and co-seismic uplift could result in three different scenarios (Figure 11c). If the co-seismic coastal uplift equals the cumulated interseismic subsidence, the coastal domain remains stable in the long term. If the former is lower than the latter, as predicted by elastic modeling (Figure 7a), the coast subsides. Conversely, the coast uplifts in the long-term if coseismic uplift ~~surpasses~~ interseismic subsidence. Considering that geological data suggest a slow coastal uplift, this last scenario should be favored but additional sources of foot-wall uplift must be identified (Ferranti *et al.*, 2006; Meschis *et al.*, 2020). At this stage, we can only evoked raw hypothesis:

- The buoyancy of the flexed Hyblean crust could significantly increase post-seismic slip after major earthquakes and thus increase footwall uplift in the coastal region.

- Further north along the coast, the Ionian slab plunges to great depth and is certainly detached from the Hyblean continental margin owing to a tear-fault propagation southward (e.g., Gutscher *et al.,* 2016; Maesano *et al.,* 2020), which could generate additional stress affecting the surface deformation of the studied region.

- Finally, the interseimic activity of the inferred extrado onshore faults alone could explain the slow long-term uplift (0.1-0.4 mm/yr) off the eastern coast of the HP. In that case, their activities should be intermittent, alternating between aseismic slip (as presently) and long periods of quiescence.

5. Conclusion

https://doi.org/10.5194/egusphere-2024-85
Preprint. Discussion started: 19 January 2024

Present-day deformation of south-eastern Sicily (Hyblean Plateau) reveals specific long and short-wavelength signals indicating a generalized eastward tilt, reversing a few kilometers before reaching the eastern coast of the Hyblean Plateau.

We propose that the long-wavelength tilt and subsidence can be explained by the flexure of the Hyblean continental crust in response to the bending force induced by the southward retreat of the Ionian subduction. Simple flexural modeling, using standard parameters (elastic thickness of 30-40 km, accretionary prism loading of 10 $N/m^2/yr$, and a local increase of bending force of 2-3.5 x10^4 N/m/yr) support this interpretation.

We show that the short wavelength coastal signal can be explained by ongoing shallow creep (at 1-4 mm/yr) of ENE trending and steeply dipping normal faults, producing the local relative uplift measured geodetically. We tested other hypotheses, such as upwelling mantle flow, volcanic deflation, and hydrological loading, and found them to be much less plausible.

Finally, we proposed that surface deformation of Southeastern Sicily is mainly controlled by bending force induced by the Ionian slab roll-back, tilting the Hyblean Plateau eastward. The bending of the continental crust causes aseismic extrados deformation along the eastern coast of the Hyblean Plateau while the normal faults, affecting the continent-ocean transition, potentially at the origin of the 1693 earthquake, remain currently locked and accumulating interseismic strain. During major earthquake, the coastal domain uplift and compensate the interseismic subsidence.

To further develop the formulated hypotheses, the acquisition of additional data is mandatory, such as: new high-resolution bathymetric data, onshore and offshore seismic data (CHIRP), on-site analysis to investigate inferred coastal active faults off Augusta-Siracusa. Besides, acquiring new PS-InSAR data would improve distinguishing geological processes from human activities. To further investigate these assumptions, perform more advanced flexural models using 3D finite element modeling techniques, and perform electri-

https://doi.org/10.5194/egusphere-2024-85
Preprint. Discussion started: 19 January 2024

cal resistivity profile and gravimetric measurements to better constrain karstic aquifers and the potential role of deep water storage and discharge on vertical surface deformation.

Competing interests:

The contact author has declared that none of the authors has any competing interests.

Acknowledgments:

This study was funded by the CNRS-INSU-Tellus programs, and the University of Montpellier (UM). Data supporting materials can be download from the Easy Data repository (Dataterra (easydata.earth)). The maps and graphics presented in this study were generated using the Generic Mapping Tools (GMT) software (Wessel and Smith, 1998). We are grateful to Serge Lallemand and Nestor Cerpa for helpful discussions on flexural models of the Ionian subduction.

Author Contributions:

Data curation: Amélie Viger, Stéphane Dominguez

Formal analysis: Amélie Viger, Stéphane Dominguez, Michel Peyret, Stéphane Mazzotti, Maxime Henriquet, Giovanni Barreca, Carmelo Monaco, Adrien Damon

Funding acquisition: Stéphane Dominguez

Ressources: Amélie Viger, Stéphane Dominguez, Maxime Henriquet, Giovanni Barreca, Carmelo Monaco

Software: Amélie Viger, Adrien Damon, Michel Peyret, Stéphane Mazzotti

Visualization: Amélie Viger, Stéphane Dominguez

Writing – original draft: Amélie Viger, Stéphane Dominguez

https://doi.org/10.5194/egusphere-2024-85
Preprint. Discussion started: 19 January 2024

Writing – review and editing: Amélie Viger, Stéphane Dominguez, Michel Peyret, Stéphane Mazzotti, Maxime Henriquet, Giovanni Barreca, Carmelo Monaco, Adrien Damon

6- References

Altamimi, Z., Rebischung, P., Métivier, L., & Collilieux, X. (2016). ITRF2014 : A new release of the International Terrestrial Reference Frame modeling nonlinear station motions. *Journal of Geophysical Research: Solid Earth*, *121*(8), 6109-6131. https://doi.org/10.1002/2016JB013098

Anzidei, M., Scicchitano, G., Scardino, G., Bignami, C., Tolomei, C., Vecchio, A., Serpelloni, E., De Santis, V., Monaco, C., & Milella, M. (2021). Relative sea-level rise scenario for 2100 along the coasts of south eastern Sicily by GNSS and InSAR data, satellite images and high-resolution topography. *EGU General Assembly Conference Abstracts*, EGU21-2889. https://ui.adsabs.harvard.edu/abs/2021EGUGA..23.2889A/abstract

APAT. (2005). *Carta geologica d'Italia Scala 1 : 1 250 000*. Agenzia per la Protezione dell'Ambiente e per i Servizi Tecnici-Dipartimento Difesa del Suolo, Servizio Geologico d'Italia., S.El.CA., Firenze, Italy. https://www.isprambiente.gov.it/images/progetti/progetto-1250-ita.jpg

Argnani, A., Armigliato, A., Pagnoni, G., Zaniboni, F., Tinti, S., & Bonazzi, C. (2012). Active tectonics along the submarine slope of south-eastern Sicily and the source of the 11 January 1693 earthquake and tsunami. *Natural Hazards and Earth System Sciences*, *12*(5), 1311-1319. https://doi.org/10.5194/nhess-12-1311-2012

Argnani, A., & Bonazzi, C. (2005). Malta Escarpment fault zone offshore eastern Sicily : Pliocene-Quaternary tectonic evolution based on new multichannel seismic data. *Tectonics*, *24*(4). https://doi.org/10.1029/2004TC001656

Azzaro, R., & Barbano, M. S. (2000). *Analysis of the seismicity of Southeastern Sicily : A proposed tectonic interpretation*. https://www.earth-prints.org/handle/2122/1292

Behncke, B. (2004). Late Pliocene volcanic island growth and flood basalt-like lava emplacement in the Hyblean Mountains (SE Sicily) : Late Pliocene Hyblean volcanism. *Journal of Geophysical Research: Solid Earth*, *109*(B9). https://doi.org/10.1029/2003JB002937

Bianca, M., Monaco, C., Tortorici, L., & Cernobori, L. (1999). Quaternary normal faulting in Southeastern Sicily (Italy) : A seismic source for the 1693 large earthquake. *Geophysical Journal International*, *139*(2), 370-394. https://doi.org/10.1046/j.1365-246x.1999.00942.x

Bigi, G., Cosentino, D., Parlotto, M., & Sartori, R. (1991). Structural model of Italy, sheet 6, 1991. *National Council of Researches Roma*.

Billi, A., Minelli, L., Orecchio, B., & Presti, D. (2010). Constraints to the cause of three historical tsunamis (1908, 1783, and 1693) in the Messina straits region, Sicily, southern Italy. *Seismological Research Letters*, *81*(6), 907-915. https://doi.org/10.1785/gssrl.81.6.907

Blewitt, G., Hammond, W., & Kreemer, C. (2018). Harnessing the GPS data explosion for interdisciplinary science. *Eos*, *99*. https://doi.org/10.1029/2018eo104623

Burgmann, R., & Thatcher, W. (2013). Space geodesy : A revolution in crustal deformation measurements of tectonic processes. *Special Paper of the Geological Society of America*, *500*, 397-430. https://doi.org/10.1130/2013.2500(12)

Canova, F., Tolomei, C., Salvi, S., Toscani, G., & Seno, S. (2012). Land subsidence along the Ionian coast of SE Sicily (Italy), detection and analysis via Small Baseline Subset (SBAS) multitemporal differential SAR interferometry. *Earth Surface Processes and Landforms*, *37*(3), 273-286. https://doi.org/10.1002/esp.2238

https://doi.org/10.5194/egusphere-2024-85
Preprint. Discussion started: 19 January 2024

Carminati, E., & Doglioni, C. (2005). Mediterranean Tectonics. In *Encyclopedia of Geology* (p. 135-146). https://doi.org/10.1016/B0-12-369396-9/00135-0

Carminati, E., Lustrino, M., & Doglioni, C. (2012). Geodynamic evolution of the central and western Mediterranean : Tectonics vs. igneous petrology constraints. *Tectonophysics*, *579*, 173-192. https://doi.org/10.1016/j.tecto.2012.01.026

Catalano, R., Doglioni, C., & Merlini, S. (2001). On the Mesozoic Ionian Basin. *Geophysical Journal International*, *144*(1), 49-64. https://doi.org/10.1046/j.0956-540X.2000.01287.x

Cavallaro, D., Monaco, C., Polonia, A., Sulli, A., & Di Stefano, A. (2017). Evidence of positive tectonic inversion in the north-central sector of the Sicily Channel (Central Mediterranean). *Natural Hazards*, *86*(S2), 233-251. https://doi.org/10.1007/s11069-016-2515-6

Chamot-Rooke, N., Rabaute, A., & Kreemer, C. (2005). Western Mediterranean Ridge mud belt correlates with active shear strain at the prism-backstop geological contact. *Geology*, *33*(11), 861. https://doi.org/10.1130/G21469.1

Chen, Y.-G., Lai, K.-Y., Lee, Y.-H., Suppe, J., Chen, W.-S., Lin, Y.-N. N., Wang, Y., Hung, J.-H., & Kuo, Y.-T. (2007). Coseismic fold scarps and their kinematic behavior in the 1999 Chi-Chi earthquake Taiwan. *Journal of Geophysical Research: Solid Earth*, *112*(B3). https://doi.org/10.1029/2006JB004388

Civello, S., & Margheriti, L. (2004). Toroidal mantle flow around the Calabrian slab (Italy) from SKS splitting. *Geophysical Research Letters*, *31*(10). https://doi.org/10.1029/2004GL019607

Cloetingh, S., Ziegler, P. A., Beekman, F., Burov, E. B., Garcia-Castellanos, D., & Matenco, L. (2015). Tectonic models for the evolution of sedimentary basins. In *Treatise on Geophysics* (p. 513-592). https://doi.org/10.1016/B978-0-444-53802-4.00117-2

Corti, G., Cuffaro, M., Doglioni, C., Innocenti, F., & Piero, M. (2006). Coexisting geodynamic processes in the Sicily Channel. In *Special Paper of the Geological Society of America* (Vol. 409, p. 96). https://doi.org/10.1130/2006.2409(05)

Cultrera, F., Barreca, G., Scarfì, L., & Monaco, C. (2015). Fault reactivation by stress pattern reorganization in the Hyblean foreland domain of SE Sicily (Italy) and seismotectonic implications. *Tectonophysics*, *661*, 215-228. https://doi.org/10.1016/j.tecto.2015.08.043

D'Agostino, N., D'Anastasio, E., Gervasi, A., Guerra, I., Nedimović, M. R., Seeber, L., & Steckler, M. (2011). Forearc extension and slow rollback of the Calabrian Arc from GPS measurements. *Geophysical Research Letters*, *38*(17). https://doi.org/10.1029/2011GL048270

D'Agostino, N., Silverii, F., Amoroso, O., Convertito, V., Fiorillo, F., Ventafridda, G., & Zollo, A. (2018). Crustal deformation and seismicity modulated by groundwater recharge of karst aquifers. *Geophysical Research Letters*, *45*(22), 12,253-12,262. https://doi.org/10.1029/2018GL079794

Dellong, D., Klingelhoefer, F., Dannowski, A., Kopp, H., Murphy, S., Graindorge, D., Margheriti, L., Moretti, M., Barreca, G., Scarfì, L., Polonia, A., & Gutscher, M. (2020). Geometry of the deep Calabrian subduction (central Mediterranean sea) from wide-angle seismic data and 3-D gravity modeling. *Geochemistry, Geophysics, Geosystems*, *21*(3), 2019GC008586. https://doi.org/10.1029/2019GC008586

Dellong, D., Klingelhoefer, F., Kopp, H., Graindorge, D., Margheriti, L., Moretti, M., Murphy, S., & Gutscher, M.-A. (2018). Crustal structure of the Ionian basin and eastern Sicily margin: results from a wide-angle seismic survey. *Journal of Geophysical Research: Solid Earth*, *123*(3), 2090-2114. https://doi.org/10.1002/2017JB015312

Fabian, A., Bruyninx, C., Miglio, A., & Legrand, J. (2021). *M3G - Metadata Management and Distribution System for Multiple GNSS Networks*. https://doi.org/10.24414/ROB-GNSS-M3G

Faccenna, C. (2005). Constraints on mantle circulation around the deforming Calabrian slab. *Geophysical Research Letters*, *32*(6), L06311. https://doi.org/10.1029/2004GL021874

Faccenna, C., Molin, P., Orecchio, B., Olivetti, V., Bellier, O., Funiciello, F., Minelli, L., Piromallo, C., & Billi, A. (2011). Topography of the Calabria subduction zone (southern Italy) : Clues for the origin of Mt. Etna. *Tectonics*, *30*(1), 2010TC002694. https://doi.org/10.1029/2010TC002694

Ferranti, L., Antonioli, F., Anzidei, M., Monaco, C., & Stocchi, P. (2010). The timescale and spatial extent of recent vertical tectonic motions in Italy : Insights from relative sea-level changes studies. *Journal of the Virtual Explorer*, *36*. https://doi.org/10.3809/jvirtex.2010.00255

Ferranti, L., Antonioli, F., Mauz, B., Amorosi, A., Dai Pra, G., Mastronuzzi, G., Monaco, C., Orrù, P., Pappalardo, M., Radtke, U., Renda, P., Romano, P., Sansò, P., & Verrubbi, V. (2006). Markers of the last interglacial sea-level high stand along the coast of Italy : Tectonic implications. *Quaternary International*, *145-146*, 30-54. https://doi.org/10.1016/j.quaint.2005.07.009

Finetti, I. R., Lentini, F., Carbone, S., Del Ben, A., Di Stefano, A., Forlin, E., Guarnieri, P., Pipan, M., & Prizzon, A. (2005). Geological outline of Sicily and lithospheric tectono-dynamics of its Tyrrhenian margin from new CROP seismic data. *CROP Project: deep seismic exploration of the central Mediterranean and Italy*, 319-375.

Frizon de Lamotte, D., Raulin, C., Mouchot, N., Wrobel-Daveau, J.-C., Blanpied, C., & Ringenbach, J.-C. (2011). The southernmost margin of the Tethys realm during the Mesozoic and Cenozoic : Initial geometry and timing of the inversion processes. *Tectonics*, *30*(3). https://doi.org/10.1029/2010TC002691

Funiciello, R., Parotto, M., Praturlon, A., & Bigi, G. (1981). Carta tettonica d'Italia alla scala 1 : 1.500. 000. *CNR Progetto Finalizzato Geodinamica, Pubbl*, *269*.

Gallen, S. F., Seymour, N. M., Glotzbach, C., Stockli, D. F., & O'Sullivan, P. (2023). Calabrian forearc uplift paced by slab–mantle interactions during subduction retreat. *Nature Geoscience*, 1-8.

Gambino, S., Barreca, G., Gross, F., Monaco, C., Gutscher, M., & Alsop, G. I. (2022). Assessing the rate of crustal extension by 2D sequential restoration analysis : A case study from the active portion of the Malta Escarpment. *Basin Research*, *34*(1), 321-341. https://doi.org/10.1111/bre.12621

Gambino, S., Barreca, G., Gross, F., Monaco, C., Krastel, S., & Gutscher, M.-A. (2021). Deformation pattern of the northern sector of the Malta Escarpment (offshore SE Sicily, Italy) : Fault dimension, slip prediction, and seismotectonic implications. *Frontiers in Earth Science*, *8*, 594176. https://doi.org/10.3389/feart.2020.594176

Goes, S., Giardini, D., Jenny, S., Hollenstein, C., Kahle, H.-G., & Geiger, A. (2004). A recent tectonic reorganization in the south-central Mediterranean. *Earth and Planetary Science Letters*, *226*(3), 335-345. https://doi.org/10.1016/j.epsl.2004.07.038

Grasso, M. t, & Lentini, F. (1982). Sedimentary and tectonic evolution of the Eastern Hyblean Plateau (Southeastern Sicily) during late Cretaceous to Quaternary time. *Palaeogeography, Palaeoclimatology, Palaeoecology*, *39*(3-4), 261-280.

Grillo, B., Braitenberg, C., Devoti, R., & Nagy, I. (2011). The study of karstic aquifers by geodetic measurements in Bus de la Genziana station – Cansiglio plateau (Northeastern Italy). *Acta Carsologica*, *40*(1). https://doi.org/10.3986/ac.v40i1.35

Gueguen, E., Doglioni, C., & Fernandez, M. (1998). On the post-25 Ma geodynamic evolution of the western Mediterranean. *Tectonophysics*, *298*(1-3), 259-269. https://doi.org/10.1016/S0040-1951(98)00189-9

Gutscher, M.-A., Dominguez, S., de Lepinay, B. M., Pinheiro, L., Gallais, F., Babonneau, N., Cattaneo, A., Le Faou, Y., Barreca, G., Micallef, A., & Rovere, M. (2016). Tectonic expression of an active slab tear from high-resolution seismic and bathymetric data offshore Sicily (Ionian Sea). *Tectonics*, *35*(1), 39-54. https://doi.org/10.1002/2015TC003898

Gutscher, M.-A., Roger, J., Baptista, M.-A., Miranda, J. M., & Tinti, S. (2006). Source of the 1693 Catania earthquake and tsunami (southern Italy) : New evidence from tsunami modeling of a locked subduction fault plane. *Geophysical Research Letters*, *33*(8). https://doi.org/10.1029/2005GL025442

Handy, M. R., M. Schmid, S., Bousquet, R., Kissling, E., & Bernoulli, D. (2010). Reconciling plate-tectonic reconstructions of Alpine Tethys with the geological–geophysical record of spreading and subduction in the Alps. *Earth-Science Reviews*, *102*(3-4), 121-158. https://doi.org/10.1016/j.earscirev.2010.06.002

Hayes, G. P., Moore, G. L., Portner, D. E., Hearne, M., Flamme, H., Furtney, M., & Smoczyk, G. M. (2018). Slab2, a comprehensive subduction zone geometry model. *Science*, *362*(6410), 58-61. https://doi.org/10.1126/science.aat4723

Henriquet, M., Dominguez, S., Barreca, G., Malavieille, J., Cadio, C., & Monaco, C. (2019). Deep origin of the dome-shaped Hyblean Plateau, Southeastern Sicily : A new tectono-magmatic model. *Tectonics*, *38*(12), 4488-4515. https://doi.org/10.1029/2019TC005548

Henriquet, M., Dominguez, S., Barreca, G., Malavieille, J., & Monaco, C. (2020). Structural and tectono-stratigraphic review of the Sicilian orogen and new insights from analogue modeling. *Earth-Science Reviews*, *208*, 103257. https://doi.org/10.1016/j.earscirev.2020.103257

Henriquet, M., Peyret, M., Dominguez, S., Barreca, G., Monaco, C., & Mazzotti, S. (2022). Present-day surface deformation of Sicily derived from Sentinel-1 InSAR time-Series. *Journal of Geophysical Research: Solid Earth*, *127*(3), Article 3. https://doi.org/10.1029/2021JB023071

Istituto Nazionale di Geofisica e Vulcanologia (INGV). (2005). *Rete Sismica Nazionale (RSN)*. https://doi.org/10.13127/SD/X0FXNH7QFY

Kreemer, C., Blewitt, G., & Klein, E. C. (2014). A geodetic plate motion and Global Strain Rate Model. *Geochemistry, Geophysics, Geosystems*, *15*(10), 3849-3889. https://doi.org/10.1002/2014GC005407

Lallemand, S., Heuret, A., Faccenna, C., & Funiciello, F. (2008). Subduction dynamics as revealed by trench migration. *Tectonics*, *27*(3), TC3014. https://doi.org/10.1029/2007TC002212

Lentini, F., & Carbone, S. (2014). Geologia della Sicilia-geology of Sicily. *Memorie Descr. Carta Geologica d'Italia*, *95*, 7-414.

Levandowski, W., Herrmann, R. B., Briggs, R., Boyd, O., & Gold, R. (2018). An updated stress map of the continental United States reveals heterogeneous intraplate stress. *Nature Geoscience*, *11*(6), 433-437. https://doi.org/10.1038/s41561-018-0120-x

Li, T., Chen, J., Thompson, J. A., Burbank, D. W., & Yang, H. (2015). Hinge-migrated fold-scarp model based on an analysis of bed geometry : A study from the Mingyaole anticline, southern foreland of Chinese Tian Shan. *Journal of Geophysical Research: Solid Earth*, *120*(9), 6592-6613. https://doi.org/10.1002/2015JB012102

Lymer, G., Lofi, J., Gaullier, V., Maillard, A., Thinon, I., Sage, F., Chanier, F., & Vendeville, B. C. (2018). The Western Tyrrhenian Sea revisited : New evidence for a rifted basin during the Messinian Salinity Crisis. *Marine Geology*, *398*, 1-21. https://doi.org/10.1016/j.margeo.2017.12.009

Maesano, F. E., Tiberti, M. M., & Basili, R. (2020). Deformation and fault propagation at the lateral termination of a subduction zone : The Alfeo Fault System in the Calabrian Arc, southern Italy. *Frontiers in Earth Science*, *8*, 107.

Masson, C., Mazzotti, S., & Vernant, P. (2019). Precision of continuous GPS velocities from statistical analysis of synthetic time series. *Solid Earth*, *10*(1), 329-342. https://doi.org/10.5194/se-10-329-2019

Mastrolembo, B., Serpelloni, E., Argnani, A., Bonforte, A., Burgmann, R., Anzidei, M., Baldi, P., & Puglisi, G. (2014). Fast geodetic strain-rates in eastern Sicily (southern Italy) : New insights into block tectonics and seismic potential in the area of the great 1693 earthquake. *Earth and Planetary Science Letters*, *404*. https://doi.org/10.1016/j.epsl.2014.07.025

Mattia, M., Bruno, V., Cannavò, F., & Palano, M. (2012). Evidences of a contractional pattern along the northern rim of the Hyblean Plateau (Sicily, Italy) from GPS data. *Geologica Acta: an international earth science journal*, *10*(1), 1-8.

Mazzotti, S., James, T. S., Henton, J., & Adams, J. (2005). GPS crustal strain, postglacial rebound, and seismic hazard in eastern North America : The Saint Lawrence valley example. *Journal of Geophysical Research: Solid Earth*, *110*(B11). https://doi.org/10.1029/2004JB003590

Meschis, M., Scicchitano, G., Roberts, G. P., Robertson, J., Barreca, G., Monaco, C., Spampinato, C., Sahy, D., Antonioli, F., Mildon, Z. K., & Scardino, G. (2020). Regional deformation and offshore crustal local faulting as combined processes to explain uplift through time constrained by investigating differentially uplifted Late Quaternary paleoshorelines : The foreland Hyblean Plateau, SE Sicily. *Tectonics*, *39*(12), e2020TC006187. https://doi.org/10.1029/2020TC006187

Michael, A. J. (1984). Determination of stress from slip data : Faults and folds. *Journal of Geophysical Research: Solid Earth*, *89*(B13), 11517-11526. https://doi.org/10.1029/JB089iB13p11517

Milano, M., Kelemework, Y., La Manna, M., Fedi, M., Montanari, D., & Iorio, M. (2020). Crustal structure of Sicily from modelling of gravity and magnetic anomalies. *Scientific Reports*, *10*(1), 16019.

Minelli, L., & Faccenna, C. (2010). Evolution of the Calabrian accretionary wedge (central Mediterranean). *Tectonics*, *29*(4). https://doi.org/10.1029/2009TC002562

Mogi, K. (1958). Relations between the Eruptions of Various Volcanoes and the Deformations of the Ground Surfaces around them. *Earthq Res Inst,* 36, 99-134.

Monaco, C., & Tortorici, L. (2000). Active faulting in the Calabrian arc and eastern Sicily. *Journal of Geodynamics*, *29*(3-5), 407-424.

Palano, M., Ferranti, L., Monaco, C., Mattia, M., Aloisi, M., Bruno, V., Cannavò, F., & Siligato, G. (2012). GPS velocity and strain fields in Sicily and southern Calabria, Italy : Updated geodetic constraints on tectonic block interaction in the central Mediterranean. *Journal of Geophysical Research: Solid Earth*, *117*(B7). https://doi.org/10.1029/2012JB009254

Prada, M., Sallarès, V., Ranero, C. R., Vendrell, M. G., Grevemeyer, I., Zitellini, N., & de Franco, R. (2014). Seismic structure of the Central Tyrrhenian basin : Geophysical constraints on the nature of the main crustal domains. *Journal of Geophysical Research: Solid Earth*, *119*(1), 52-70.

Rabaute, A., & Chamot-Rooke, N. (2019). Active inversion tectonics from Algiers to Sicily. In N. Sundararajan, M. Eshagh, H. Saibi, M. Meghraoui, M. Al-Garni, & B. Giroux (Éds.), *On Significant Applications of Geophysical Methods* (p. 249-251). Springer International Publishing. https://doi.org/10.1007/978-3-030-01656-2_56

Ridente, D., Martorelli, E., Bosman, A., & Chiocci, F. L. (2014). High-resolution morpho-bathymetric imaging of the Messina Strait (Southern Italy). New insights on the 1908 earthquake and tsunami. *Geomorphology*, *208*, 149-159. https://doi.org/10.1016/j.geomorph.2013.11.021

Rosenbaum, G., Lister, G. S., & Duboz, C. (2002). Reconstruction of the tectonic evolution of the western Mediterranean since the Oligocene. *Journal of the Virtual Explorer*.

Rovida, A., Locati, M., Camassi, R., Lolli, B., Gasperini, P., & Antonucci, A. (2022). *Catalogo Parametrico dei Terremoti Italiani (CPTI15), versione 4.0* (4.0, p. 4894 earthquakes). Istituto Nazionale di Geofisica e Vulcanologia (INGV). https://doi.org/10.13127/CPTI/CPTI15.4

Scandone, P., Patacca, E., Radoicic, R., Ryan, W. B. F., Cita, M. B., Rawson, M., Chezar, H., Miller, E., McKenzie, J., & Rossi, S. (1981). Mesozoic and Cenozoic rocks from Malta escarpment (central Mediterranean). *AAPG Bulletin*, *65*(7), 1299-1319.

Scarfì, L., Barberi, G., Barreca, G., Cannavò, F., Koulakov, I., & Patanè, D. (2018). Slab narrowing in the Central Mediterranean : The Calabro-Ionian subduction zone as imaged by high resolution seismic tomography. *Scientific Reports*, *8*(1), Article 1. https://doi.org/10.1038/s41598-018-23543-8

Schmincke, H.-U., Behncke, B., Grasso, M., & Raffi, S. (1997). Evolution of the northwestern Iblean Mountains, Sicily : Uplift, Plicocene/Pleistocene sea-level changes, paleoenvironment, and volcanism. *Geologische Rundschau*, *86*, 637-669.

Scicchitano, G., Antonioli, F., Berlinghieri, E. F. C., Dutton, A., & Monaco, C. (2008). Submerged archaeological sites along the Ionian coast of Southeastern Sicily (Italy) and implications for the Holocene relative sea-level change. *Quaternary Research*, *70*(1), 26-39. https://doi.org/10.1016/j.yqres.2008.03.008

Scicchitano, G., Gambino, S., Scardino, G., Barreca, G., Gross, F., Mastronuzzi, G., & Monaco, C. (2022). The enigmatic 1693 AD tsunami in the eastern Mediterranean Sea : New insights on the triggering mechanisms and propagation dynamics. *Scientific Reports*, *12*(1), 9573. https://doi.org/10.1038/s41598-022-13538-x

Scognamiglio, L., Tinti, E., & Quintiliani, M. (2006). *Time Domain Moment Tensor (TDMT)* [jeu de données]. Istituto Nazionale di Geofisica e Vulcanologia (INGV). https://doi.org/10.13127/TDMT

Sgroi, T., De Nardis, R., & Lavecchia, G. (2012). Crustal structure and seismotectonics of central Sicily (southern Italy) : New constraints from instrumental seismicity: Seismotectonics of central Sicily. *Geophysical Journal International*, *189*(3), 1237-1252. https://doi.org/10.1111/j.1365-246X.2012.05392.x

Silverii, F., D'Agostino, N., Métois, M., Fiorillo, F., & Ventafridda, G. (2016). Transient deformation of karst aquifers due to seasonal and multiyear groundwater variations observed by GPS in southern Apennines (Italy). *Journal of Geophysical Research: Solid Earth*, *121*(11), 8315-8337. https://doi.org/10.1002/2016JB013361

Spampinato, C. R., Braitenberg, C., Monaco, C., & Scicchitano, G. (2013). Analysis of vertical movements in eastern Sicily and southern Calabria (Italy) through geodetic leveling data. *Journal of Geodynamics*, *66*, 1-12. https://doi.org/10.1016/j.jog.2012.12.002

Speranza, F., Minelli, L., Pignatelli, A., & Chiappini, M. (2012). The Ionian Sea : The oldest in situ ocean fragment of the world?: MAGNETIC MODELLING OF THE IONIAN SEA. *Journal of Geophysical Research: Solid Earth*, *117*(B12), n/a-n/a. https://doi.org/10.1029/2012JB009475

Stampfli, G. M., Borel, G. D., Marchant, R., & Mosar, J. (2002). Western Alps geological constraints on western Tethyan reconstructions. *Journal of the Virtual Explorer*, *08*. https://doi.org/10.3809/jvirtex.2002.00057

Stephenson, O. L., Liu, Y.-K., Yunjun, Z., Simons, M., Rosen, P., & Xu, X. (2022). The Impact of Plate Motions on Long-Wavelength InSAR-Derived Velocity Fields. *Geophysical Research Letters*, *49*(21), e2022GL099835. https://doi.org/10.1029/2022GL099835

Tesauro, M., Audet, P., Kaban, M. K., Bürgmann, R., & Cloetingh, S. (2012). The effective elastic thickness of the continental lithosphere : Comparison between rheological and inverse approaches. *Geochemistry, Geophysics, Geosystems*, *13*(9). https://doi.org/10.1029/2012GC004162

Toda, S., Stein, R. S., Sevilgen, V., & Lin, J. (2011). Coulomb 3.3 Graphic-rich deformation and stress-change software for earthquake, tectonic, and volcano research and teaching—User guide. *US Geological Survey open-file report*, *1060*(2011), 63.

Trua, T., Serri, G., & Marani, M. P. (2003). Lateral flow of African mantle below the nearby Tyrrhenian plate : Geochemical evidence. *Terra Nova*, *15*(6), 433-440. https://doi.org/10.1046/j.1365-3121.2003.00509.x

Tugend, J., Chamot-Rooke, N., Arsenikos, S., Blanpied, C., & Frizon De Lamotte, D. (2019). Geology of the Ionian Basin and Margins : A Key to the East Mediterranean Geodynamics. *Tectonics*, *38*(8), 2668-2702. https://doi.org/10.1029/2018TC005472

Turcotte, D. L., & Schubert, G. (2014). *Geodynamics* (Third edition). Cambridge University Press.

Van Hinsbergen, D. J. J., Torsvik, T. H., Schmid, S. M., Maţenco, L. C., Maffione, M., Vissers, R. L. M., Gürer, D., & Spakman, W. (2020). Orogenic architecture of the Mediterranean region and kinematic reconstruction of its tectonic evolution since the Triassic. *Gondwana Research*, *81*, 79-229. https://doi.org/10.1016/j.gr.2019.07.009

Vavryčuk, V. (2014). Iterative joint inversion for stress and fault orientations from focal mechanisms. *Geophysical Journal International*, *199*(1), 69-77. https://doi.org/10.1093/gji/ggu224

ViDEPI. (s. d.). https://www.videpi.com/videpi/videpi.asp

Vilardo, G., Ventura, G., Terranova, C., Matano, F., & Nardò, S. (2009). Ground deformation due to tectonic, hydrothermal, gravity, hydrogeological, and anthropic processes in the Campania Region (Southern Italy) from Permanent Scatterers Synthetic Aperture Radar Interferometry. *Remote Sensing of Environment*, *113*(1), 197-212. https://doi.org/10.1016/j.rse.2008.09.007

Vollrath, A., Zucca, F., Bekaert, D., Bonforte, A., Guglielmino, F., Hooper, A., & Stramondo, S. (2017). Decomposing DInSAR time-series into 3-D in combination with GPS in the case of low strain rates : An application to the Hyblean Plateau, Sicily, Italy. *Remote Sensing*, *9*(1), 33. https://doi.org/10.3390/rs9010033

Watts, A. B., & Zhong, S. (2000). Observations of flexure and the rheology of oceanic lithosphere. *Geophysical Journal International, 142(3)*, 855-875.

Wells, D. L., & Coppersmith, K. J. (1994). New empirical relationships among magnitude, rupture length, rupture width, rupture area, and surface displacement. *Bulletin of the seismological Society of America*, *84*(4), 974-1002.

Wessel, P., & Smith, W. H. F. (1998). New, improved version of generic mapping tools released. *Eos, Transactions American Geophysical Union*, *79*(47), 579-579. https://doi.org/10.1029/98EO00426

Wickert, A. D. (2016). Open-source modular solutions for flexural isostasy : gFlex v1.0. *Geoscientific Model Development*, *9*(3), 997-1017. https://doi.org/10.5194/gmd-9-997-2016

Wortel, M. J. R., & Spakman, W. (2000). Subduction and Slab Detachment in the Mediterranean-Carpathian Region. *Science*, *290*(5498), 1910-1917. https://doi.org/10.1126/science.290.5498.1910